Covalent Mechanochemistry and Contemporary Polymer Network Chemistry: A Marriage in the Making

Authors: Evan M. Lloyd,[1] Jafer R. Vakil,[1,2] Yunxin Yao,[1,2] Nancy R. Sottos[2,3] and Stephen L. Craig[1,2*]

Affiliation:

[1]Department of Chemistry, Duke University, Durham, NC 27708, United States

[2]NSF Center for the Chemistry of Molecularly Optimized Networks, Duke University, Durham, NC 27708, United States

[3]Department of Materials Science and Engineering, University of Illinois, Urbana, IL 61801, United States

*Email: stephen.craig@duke.edu

Abstract: Over the last twenty years, the field of polymer mechanochemistry has amassed a toolbox of mechanophores that translate mechanical energy into a variety of functional responses ranging from color change to small molecule release. These productive chemical changes typically occur at the length scale of a few covalent bonds (Å), but require large energy inputs and strains on the micro-to-macro scale in order to achieve even low levels of mechanophore activation. The minimal activation hinders the translation of the available chemical responses into materials and device applications. The mechanophore activation challenge inspires core questions at yet another length scale of chemical control, namely: What are the molecular-scale features of a polymeric material that determine the extent of mechanophore activation? Further, how do we marry advances in the chemistry of polymer networks with the chemistry of mechanophores to create stress-responsive materials that are well suited for an intended application? In this Perspective, we speculate as to the potential match between covalent polymer mechanochemistry and recent advances in polymer network chemistry, specifically, topologically controlled networks and the hierarchical material responses enabled by multinetwork architectures and mechanically interlocked polymers. Both fundamental and applied opportunities unique to the union of these two fields are discussed.

1. INTRODUCTION

Recent advances in polymer mechanochemistry have revolutionized the way we view extrinsic mechanical forces in polymeric materials (Figure 1). Once seen as an almost purely destructive form of energy, mechanical force is now a recognized stimulus that can drive productive chemical transformations. The force coupled modification of potential energy landscapes has been used for stress-induced material transformations,[1–6] classically forbidden reaction pathways,[7,8] and biased product formation.[9,10] Since Berkowski and coworkers reported the site-specific chain scission of azo-centered poly(ethylene glycol) in 2005,[11] the field of polymer mechanochemistry has burgeoned to include contributions from chemists and engineers across the world. Nearly two decades later, this rapidly developing field has amassed a library of mechanoresponsive units, known colloquially as mechanophores, with a myriad of functions including radical generation,[12,13] small molecule release,[14–21] molecular stress relief,[22–28] color changes and luminescence,[29–35] and catalyst activation.[36–38] Polymer mechanochemistry has successfully been applied at length scales from single polymer strands[39] to structured metamaterials[40] and in a variety of material systems.[41] For a deeper dive into the rich history of polymer mechanochemistry, we direct our readers to several recent review articles.[41–45]

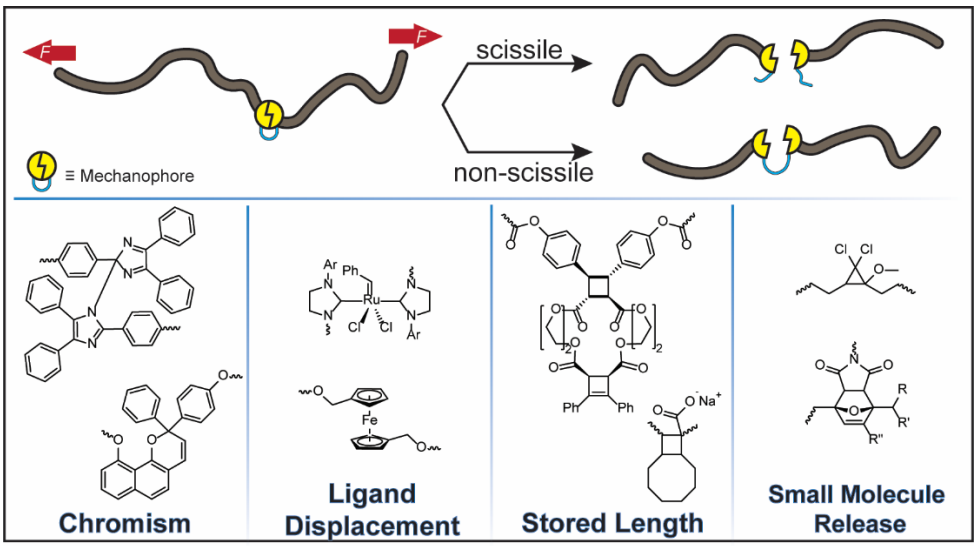

Figure 1. The mechanophore concept and selected toolbox of responses.

For many of us, our forays into polymer mechanochemistry began with the characterization of mechanochemical reactions in linear polymers with single-molecule force spectroscopy[46] and solution-state ultrasonication.[39] We are increasingly drawn, however, to what we see as a potentially transformative goal: translating the responses observed in isolated molecules to bulk materials made from polymer networks. Our endeavors in this area have often realized low (~ 0.1 – 1%) levels of activated response among the mechanophores embedded within polymer networks, despite high levels of activation during solution-state measurements.[15,47,48] These low levels of activation challenge the translation of polymer mechanochemistry into materials centered applications, and they have forced us to (repeatedly) speculate as to why mechanophore activation is often so inefficient in bulk materials, as well as what we might do to improve it. In this Perspective, we share some of those speculations.

A little history might provide some useful context. We and several of our colleagues in the field have attempted several molecular and materials engineering approaches (Figure 2a) to improve mechanophore activation in bulk systems with varying success. Some gains are possible at the level of molecular engineering. Robb and coworkers investigated the impact of polymer attachment points in naphthopyran-laden silicone elastomers.[49] Regioisomers with polymer attachment at the 5-position of naphthopyran efficiently transmit tension along the target C-O pyran bond and samples turn a deep yellow upon stretching (Figure 2b). Those attached at the 8- or 9-position do not exhibit mechanochromism in the bulk. Similarly, we explored regiochemical effects on spiropyran activation in silicone elastomers and found that *ortho* substitution leads to a greater colorimetric response, consistent with theoretical predictions based purely on molecular architecture (Figure 2c).[50] Even for the same attachment point, work on ferrocene derivatives revealed that the ability of the mechanophore to undergo force-coupled conformational changes prior to scission influences both the mechanism and probability of reaction when the mechanophores are embedded in an otherwise identical polymer network.[17,51] Where the magnitude of the response differs with molecular substitution pattern, the macroscopic strain necessary for measurable

mechanophore activation, however, is often constant.[52] Molecular engineering impacts the level of interaction, but appears to do so within bounds that are set by the surrounding network architecture.

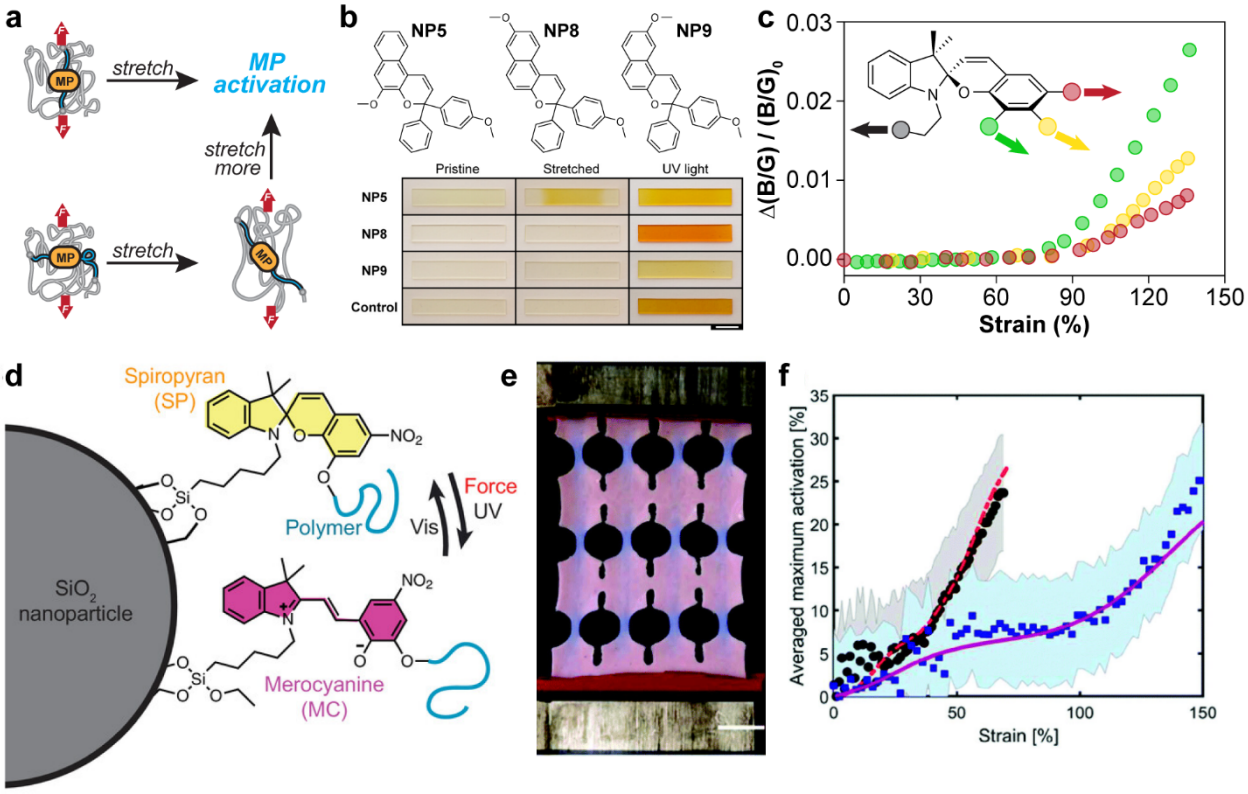

Figure 2. Methods of improving mechanophore activation in conventional polymer networks. a) Schematic demonstrating the importance of mechanophore orientation for activation in polymer networks. b) Activation of naphthopyran regioisomers in PDMS elastomers. Mechanical activation is only observed in NP5 regioisomer. c) Activation of three different spiropyran regioisomers in PDMS elastomers. All three isomers show similar onsets of activation, but *ortho*-spiropyran exhibits enhanced mechanochromism. d) Schematic representation of spiropyran activation at the interface between silica nanoparticles and the bulk polymer network. e) Optical image of spiropyran activation in architected lattice. f) Averaged maximum spiropyran activation vs. macroscopic strain in lattice (black circles) and traditional materials (blue squares). Image (b) adapted with permission from Ref. 49 Copyright 2016 American Chemical Society. Image (c) adapted with permission from Ref. 50. Copyright 2018 American Chemical Society. Image (d) adapted with permission under a Creative Commons CC BY 4.0 License from Ref. 53. Copyright 2020 John Wiley and Sons. Images (e), (f) reproduced with permission from Ref. 40. Copyright 2020 Royal Society of Chemistry.

Various approaches to engineering the surrounding network environment have centered on introducing anisotropy (e.g., through chain alignment, particle interfaces, or architected structures) into materials. Beiermann and coworkers found that when spiropyran is embedded within the backbone of a linear polymer, activation improves as the polymer chains align with the applied strain.[54,55] By increasing the strain rate, they increased alignment of poly(methyl acrylate) chains, leading to superior activation. Weng and coworkers utilized ureidopyrimidinone (UPy) hydrogen bonding motifs to promote chain alignment and strain induced crystallization,[56,57] leading to five-fold enhancements in the overall extent of activation. Kim and coworkers synthesized elastomeric nanocomposites with spiropyran located at the nanoparticle-polymer interface (Figure 2d).[53] The stress concentrations at the heterointerface resulted in greater spiropyran activation and significantly decreased activation onsets relative to mechanophores in the bulk matrix. Schwartz and coworkers expanded engineering approaches to include macroscopically architected materials.[40] Periodic lattices made from mechanochromic silicone elastomers decreased the activation onset strain by a factor of two from that of unstructured, bulk samples. Each of these approaches represent significant advances in bulk polymer mechanochemistry, but they still fall short of the activation efficiencies seen in single polymer chain and solution state experiments.

In this Perspective, we explore some of the key molecular features limiting mechanophore activation at network levels. We dive into the topological features which influence the molecular tension distributions and ultimate properties of elastomeric materials. We then provide a brief review of recent progress in the design of polymer network architectures,

emphasizing networks with controlled topology or hierarchical structure. Finally, we discuss the opportunities for improved mechanophore activation by marrying polymer mechanochemistry with contemporary, molecular based polymer network design.

2. ACTIVATION OF MECHANOPHORES

The mechanophore is an effective tool for mechanochemical transduction. In solution-state and single-molecule force spectroscopy (SMFS) measurements, very high levels of mechanochemical activity are possible. In our own work, we have observed greater than 60% activation of various multi-mechanophore systems during pulsed ultrasound experiments.[7,15,39,58–60] This value is typically limited by competitive scission of polymer chains in the presence of large shear forces, which reduces the polymer chain length below the critical threshold for activation during pulsed ultrasound.[61] Similarly, quantitative mechanophore activation (hundreds or even thousands of non-scissile events along a single polymer molecule) are possible during a single SMFS experiment.[17,22,61–64] Others have also demonstrated similar levels of activation in systems with a wide range of force-coupled kinetics.[16,63,65,66] Given that mechanochemical transduction is incredibly efficient during extension of single polymer chains, why does mechanophore activation in polymer networks remain such a challenge? We here turn our attention to mechanophore activation at the bulk level and direct the reader to several review articles for more information on solution-state and SMFS experiments.[41,44,67]

Most bulk systems exhibit very low levels of mechanophore activation even after sustaining large, often irreversible, strains.[53,68,69] One our first endeavors into bulk mechanochemistry resulted in less than 0.1 % activation during unconstrained uniaxial compression of a *gem*-dichlorocycloproponated polybutadiene (gDCC-PB),[47] despite the fact that more than 80% of gDCC mechanophores ring open during ultrasonication[39] Similarly, hammering a silicone elastomer with a 2-methoxy-substituted *gem*-dichlorocyclopropane (MeO-gDCC) mechanoacid incorporated into the crosslinks yields only ~0.2 % activation, where greater than 60% activation is possible by ultrasonication of a MeO-gDCC containing linear polymer.[15] Further, Davis and coworkers found that during uniaxial tension, nearly 200% strain is required for the onset of spiropyran activation in poly(methyl acrylate) elastomers and that significant optical response was not observed until at least 500% strain.[1] The onset of spiropyran activation is reduced to less than 100% strain in silicone elastomers, but only small color changes are observed prior to failure of the network.[50,52] These marginal levels of mechanochemical transduction are common amongst bulk networks,[20,70] and we believe that they are a direct consequence of the topology of traditional polymer networks.

The techniques utilized to prepare traditional polymer networks, such as addition polymerization or vulcanization, offer little control over the network topology, and subsequently, most polymer networks are marked by a large degree of heterogeneity and a variety of topological features.[71–73] First, the uncontrolled polymerization or crosslinking processes produce a wide range of polymer chain lengths between crosslinks. Theoretical depictions of network formation suggest a non-uniform distribution of strand lengths,[74] where the concentration of short chains greatly influences the elasticity and the ultimate strength of the network.[75,76] Additionally, scattering experiments[77–80] have shown localized heterogeneities in polymer strand and crosslink densities, which arise from spatiotemporal fluctuations in monomer concentration during synthesis[81] and are known to influence the local elastic environment.[82] The effective crosslink density is also influenced by molecular entanglements, as the presence of chemical crosslinks prevents the disentanglement of polymer strands.[83] These physical entanglements contribute significantly to the elasticity and strength of a polymer network.[84,85] Finally, topological defects, such as closed loops or dangling chains, result in elastically ineffective chains, and network stiffness decreases with increasing defect concentrations.[84,86,87] These topological heterogeneities all contribute to a non-uniform distribution of tension in strained network strands.

In classical models of polymer chain elasticity, force is dependent on the ratio of end-to-end distance and contour length. Therefore, in an elastomeric network, the distribution of tension has been proposed to depend on the strand length dispersity, where, on average, short and long strands experience larger and smaller forces, respectively.[88,89] This and other factors are expected to result in a very broad tension distribution that has a long tail extending into high forces.[88–91] Simulations reported by Adhikari and Makarov suggest, for example, that the high-force tails may take the form of an exponential force distribution, with an observable portion of strands experiencing tension that is six to eight times greater than the average force within the network.[90] The topology described by the relative contributions of entanglements and covalent cross-linking influenced the details of the distribution. We anticipate that other topological features (e.g., local fluctuations in crosslink density and some of the topologies described in Section 3) will further contribute to the specifics of molecular force distributions and, subsequently, to the extent of mechanochemical transduction.

The tension distribution has direct consequences for the level of mechanochemical response. For mechanophores that react via a unimolecular process, the total intensity I of mechanochemical response in a polymer network that is stretched to a given strain is given by:

$$I \propto \frac{\int_0^\infty p(F)G(F)dF}{\int_0^\infty p(F)dF}$$

Where $p(F)$ is the probability density that captures the molecular force distribution that results from the strain, and $G(F) = 1 - \exp[k(F)t]$ is the probability that a mechanophore will have reacted when experiencing force F over the time t that the strain-generated force is experienced. The probability $G(F)$ depends on the force-coupled rate constant $k(F)$ of the reaction of interest. At the molecular level, the coupling of tension to a reactant modifies the potential energy landscape, including a change in the activation barrier of a chemical reaction. The true force-rate dependence can be quite complicated[92–96], but in the simplest cases the force-coupled reaction kinetics are reasonably approximated by:

$$k(F) \propto e^{-(\Delta E_A - F\Delta x)/RT}$$

where k, F, ΔE_A, Δx, R, and T respectively refer to the reaction rate, applied external force, force-free activation energy, activation length, universal gas constant, and temperature.[68,88] A key point is that rate is not proportional to force, and so the average rate across an ensemble is not necessarily equal to the rate at the average force of the ensemble, and doubling the stress in a material does not necessarily have an effect on I that is proportional to the effect of doubling force on $G(F)$. An understanding of $p(F)$, and how its strain-dependence is related to the molecular details of network topology, is as critical to the material-level implementation of mechanophores as is an understanding how the molecular aspects of mechanophore design dictate $k(F)$ and therefore $G(F)$. [90] This includes that fraction of mechanophores embedded within elastically ineffective strands, which will remain unloaded and unactivated regardless of the external load applied.

When $p(F)$ is broad, polymer strands at the high-force end of the distribution will start to break (for example, through homolytic scission) at significant levels even as the vast majority of strands are under tension that is too low to trigger a mechanochemical response of interest (Figure 3). In other words, the maximum achievable I is limited by the form of $p(F)$, because of the competition between the desired mechanophore activation and undesired force-coupled strand scission that increases the stress on neighboring strands,[97,98] which are then more likely to fail in a catastrophic cascading fashion[89] at strains well below the maximum theoretical value.[99,100] That competition presents an opportunity for internal feedback. With non-scissile mechanophores, the polymer contour length increases upon activation, a process we have come to call reactive strand extension,[63,101] and there is an associated relief of stress as slack is released during the mechanochemical reaction. In other words, force-coupled reactions can change $p(F)$ without chain scission. We note, however, that reactive strand extension in most systems is small[22] and further mechanophore development is likely needed to decipher the relationship between strand extension and $p(F)$.

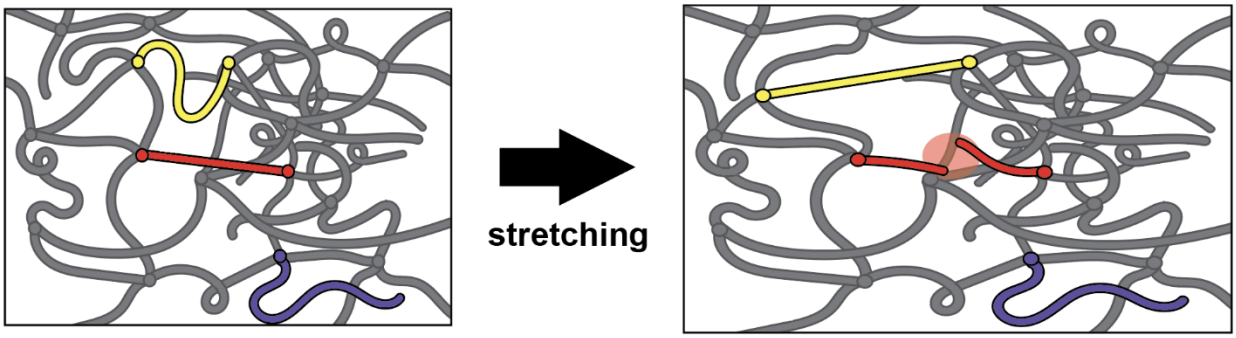

Figure 3. Schematic depiction of a distribution of relative strand tension and orientation in a network and how these strands respond to the same macroscopic deformation. Certain loose strands (yellow) may become taut under tension, other strained strands (red) may break, and other strands (purple) may remain inert to such deformations.

3. CONTEMPORARY NETWORK DESIGN

A broad and open question, then, is how the fundamental limits of tailing force distributions and premature network failure of conventional networks might be addressed through contemporary polymer network chemistry, and the extent to which network chemistry can be optimized to enhance mechanochemical transduction in bulk materials. Specific opportunities include advances in our characterization and understanding of polymer network topology, the development of mechanically interlocked polymers, and multinetwork materials. The polymer chemistry being developed for each of these areas holds consequences for the distribution of tension felt within strands in a given network. Advances in network topological characterization and control should inform molecular-scale structure activity relationships in traditional, fixed single networks. The conformational degrees of freedom present in mechanically interlocked polymers enable redistribution of stress and reorganization of networks at low forces. Finally, by incorporating efficient energy dissipation and load transfer mechanisms, multinetwork materials delay the onset of failure following covalent bond rupture. Each aspect of network architecture carries potential consequences for the extent of activation of embedded mechanophores and the contribution of their response to material properties.

3.1 Topologically controlled networks

Many topological heterogeneities present in conventional polymer networks are intrinsic to the nature of polymerization processes themselves.[72] For example, traditional polymerization processes, such as free radical polymerization, are often marked by slow initiation, rapid propagation, and extensive transfer or termination. With slow initiation and rapid propagation, polymerization occurs in localized clusters, and the spatial density of polymer strands and crosslinks fluctuates significantly as the network forms (Figure 4a). Termination or transfer of propagating strands yields dangling chain ends, and intramolecular cyclization forms loop defects, both reducing the elasticity of the network. Finally, for some networks at late stages of network formation, clusters become concentrated, and generated radicals link them together to form the final heterogeneous material.[72] Homogeneous network synthesis, therefore, requires well-controlled strategies such as living polymerization or end-linking of polymeric precursors with defined structure to prevent localized polymerization clusters. In recent years, more exotic approaches, such as biasing polymerization kinetics[102] or templated syntheses,[103] have also been leveraged to modulate topology.

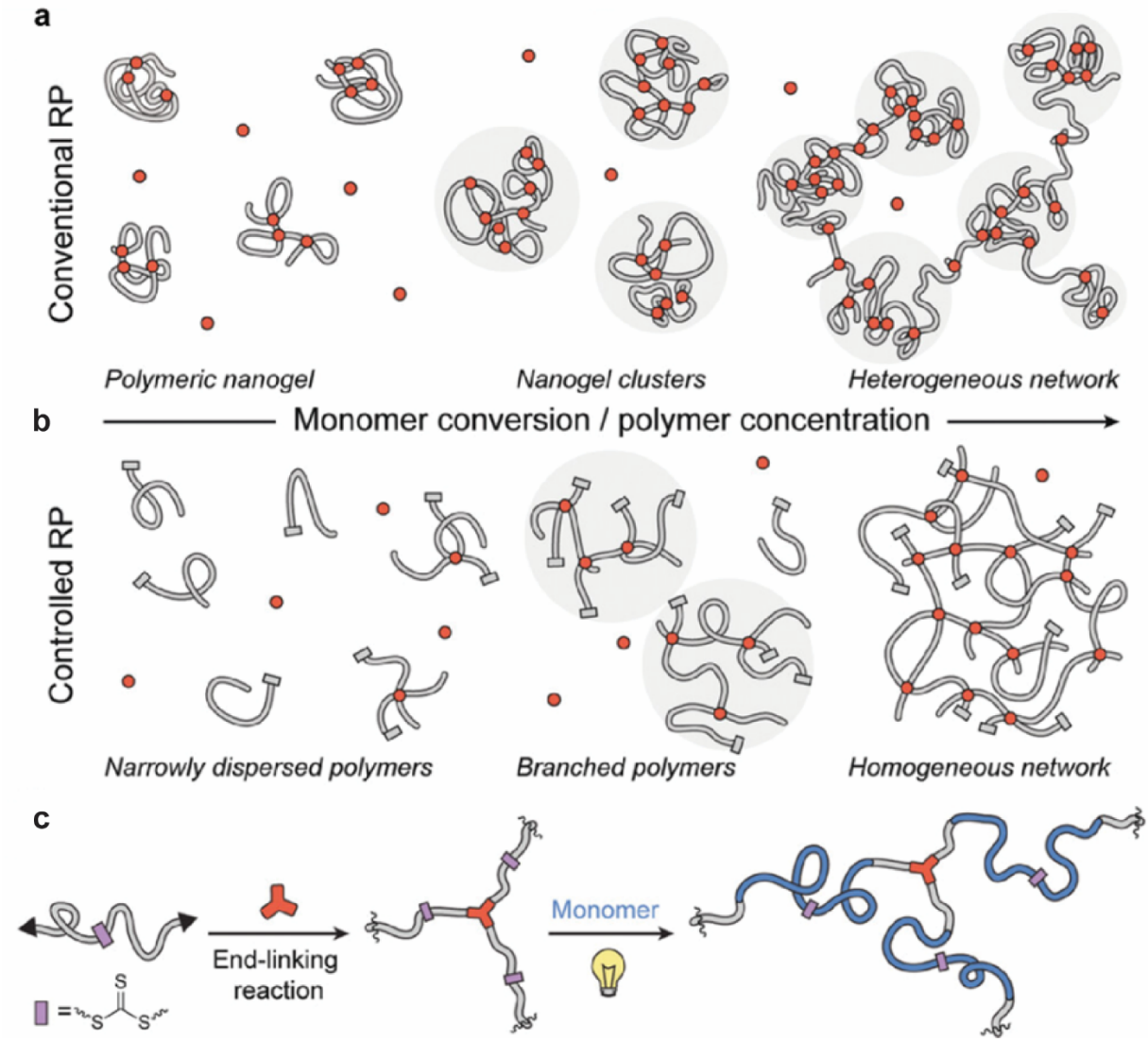

Figure 4. Strategies for network preparation. a) Formation of heterogeneous networks by conventional free-radical polymerization. b) Synthesis of less heterogeneous networks by controlled radical polymerization. c) Endlinking of polymeric precursors with a multifunctional crosslinker. Images (a–c) adapted with permission from Ref.72. Copyright 2020 John Wiley and Sons.

Living polymerization methods are characterized by rapid initiation, slow propagation, and minimal transfer or termination.[104,105] Rapid initiation ensures that growing polymer chains are homogeneously distributed throughout the

forming network, while slow propagation ensures that monomers or crosslinkers are added to all growing chains at a relatively uniform rate (Figure 4b). Further, with slow propagation, the growing strands are free to diffuse, preventing the concentration and linking of clusters in localized regions.[106,107] The resulting homogeneous networks display properties that are vastly different from those prepared through conventional polymerization techniques. Several groups have observed higher degrees of swelling and more rapid release kinetics in hydrogels prepared through reversible addition-fragmentation chain transfer polymerization or atom transfer radical polymerization than those prepared through conventional free radical polymerization.[108–110] When utilizing nitroxide-controlled free radical polymerization, Ide and Fukuda reported gelation that was consistent with Flory and Stockmayer gelation theory.[106] In comparison, critical crosslink density at gelation reported for uncontrolled radical addition systems is often one or two orders of magnitude larger than theoretical predictions.[106] For additional insights into network formation through living polymerization, we direct the readers to a review article by Moad.[107]

The exquisite control over molecular weight, chain-end functionality, and architecture afforded by living polymerization methods[104,105,111] has also greatly influenced end-linking strategies for network preparation. As discussed previously, a key feature of any living polymerization is the relatively fast initiation compared to propagation, which leads to relatively narrow molecular weight distributions ($Đ < 1.4$). Further, by maintaining a constant number of propagating chains, one can accurately predict and control the molecular weight of the final polymer by simply adjusting the initial monomer to initiator ratio.[112,113] Also, the chain ends in a living polymerization are precisely defined by the selected initiating and terminating species,[105] and telechelic polymers are easily obtained through modification of the chain ends.[114] End-linking of these structurally-defined polymeric precursors with multifunctional junctions (i.e. crosslinkers), often through click chemistry,[86,114,115] precludes the formation of heterogeneous clusters, and homogeneous topologies are obtained (Figure 4c). While these networks are not free of defects, end-linking provides a different level of control over network topology than conventional methods.[116,117]

The branch functionality of junctions has also been shown to greatly influence network topology and properties. Via Monte Carlo simulations, Wang and coworkers demonstrated an interesting odd-even effect of junction functionality on the concentration of primary loops: odd junction functionality values led to higher concentrations of elastically ineffective primary loops while even junction functionality yielded more secondary loops.[118] They also observed that higher order functionality led to greater shear moduli in phantom networks. Johnson and coworkers similarly found that higher order functionality resulted in stiffer networks when working with metal-organic cage junctions.[119,120] They attributed these results to the defect tolerance of networks with high functionality junctions.

The Johnson group has pioneered additional methods to control network topology, including semibatch monomer addition[102] and templated syntheses.[103] They found that by slowly adding a four-arm star polymer crosslinker (B_4) into an excess of bifunctional monomer (A_2) until near the gel point and then quickly adding the amount of B_4 required to reach 1:1 stoichiometry, they drastically reduced the primary loop content.[102] Adjusting the rate of B_4 titration in the initial slow addition phase precisely tuned the primary loop concentration, and the resulting crosslinked gels demonstrated shear storage moduli up to 600% greater than when conventional batch mixing was utilized. Similar results were obtained at different A and B component functionalities. In a separate publication, they modified four-arm star polymers with long alkyl chains to promote self-assembly of the hydrophobic precursors prior to gel formation.[103] Introduction of a bis-potassium acyltrifluoroborate oligomer induced amide bond formation and cleavage of the alkyl chain leaving groups. Templated self-assembly prior to network formation resulted in densely crosslinked nanoclusters and a heterogeneous structure. When short alkyl chains were utilized, no self-assembly was observed, and the resulting gels were topologically homogeneous.

Our understanding of the interplay of synthetic methods with network topology, and the consequences of topology on mechanochemical transduction, will be accelerated by the development of direct chemical methods for characterizing molecular-scale distribution of network topology. To this end, the network disassembly spectrometry (NDS) technique recently developed by Johnson and co-workers is particularly enabling.[72] NDS allows precise quantification of topological characteristics by introducing chemical labels and designed cleavage sites into the network. Deconstruction through triggered cleavage yields soluble fragments, often with isotopic labels, which can be analyzed by traditional spectroscopic methods. NDS has been successful in quantifying the number of primary and secondary loops and dangling chain ends in soft polymeric networks[86,102,103,114,121–125] as well as the extent of crosslinking in high glass transition temperature thermosets.[126]

3.2 Mechanically interlocked polymers

Unique to mechanically interlocked polymers (MIPs) is the presence of a mechanical bond (Figure 5a). Unlike covalent bonds which fix molecules together permanently at a precise position, mechanical bonds permit linked molecular components to sample much larger spaces.[127] Subsequently, mechanically interlocked polymers are characterized by significant translational, rotational, elongational, and torsional degrees of freedom. Mechanical bonds take a variety of different forms, but the most common types of MIPs comprise main-chain polyrotaxanes (simply referred to as

polyrotaxanes), slide-ring materials (a subclass of polyrotaxanes), and polycatenanes. For a comprehensive discussion of MIPs, we direct the readers to a review article from Hart and coworkers.[127]

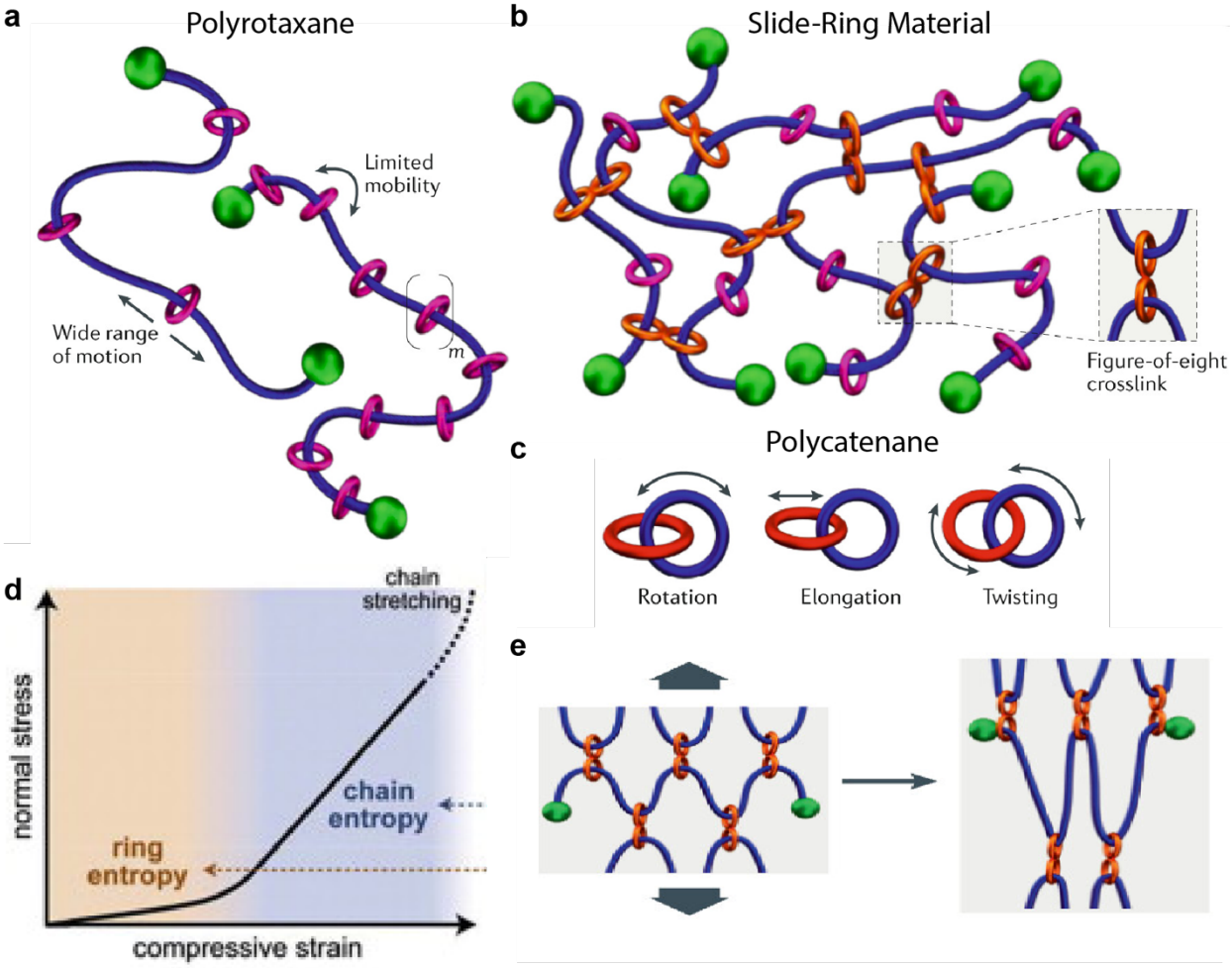

Figure 5. Mechanically interlocked polymers. A-c) Structures of various MIPs and depictions of their mobility. D) Schematic representation of stress-strain response for a slide-ring material. Initial strain is dominated by entropic elasticity from the translation of rings and characterized by a large force-coupled displacement. E) Redistribution and equalization of stress in a slide-ring material under tension. Images (a-c) adapted by permission from Springer Nature Customer Service Centre GmbH: Springer Nature, Nature Review Materials, Material properties and applications of mechanically interlocked polymers, Laura F. Hart et al., Copyright (2021).[127] Image (d) reprinted from Polymer, 55(10), Kazuaki Kato et al., Peculiar elasticity and strain hardening attributable to counteracting entropy of chain and ring in slide-ring gels, 2614-2619, Copyright (2014), with permission from Elsevier.[128]

In polyrotaxanes, macrocyclic rings are free to rotate and slide along a polymer backbone until their motion is frustrated by contact with additional rings or bulky substituents placed at the ends of or along the polymer backbone. The properties of polyrotaxanes are easily tuned by controlling the chemical properties of each individual component as well as translational freedom of the rings, which is dictated by ring and stopper density.[127] Polyrotaxanes are typically synthesized by the complexation of macrocyclic rings with a suitable polymer chain, followed by the addition of bulky stoppers to trap the rings.[129] Complexation is driven by favorable intermolecular interactions between the macrocycle and the polymer chain and between neighboring macrocycles.[130] Slide-ring materials (SRMs) represent the network analogue of polyrotaxanes. Similar to polyrotaxanes, they benefit from large translational freedom which is controlled by the density of slide-rings and stoppers as well as intermolecular interactions. SRMs were initially proposed theoretically by de Gennes in 1999[131], but they were not realized experimentally until two years later when Okumura and Ito synthesized a polyrotaxane gel with figure-of-eight crosslinks.[132] Since their introduction, SRM synthesis has been dominated by covalently crosslinking the macrocyclic rings of preformed polyrotaxanes.[133–135] A related class of mechanically

interlocked polymers, polycatenanes, do not possess the long-range translational freedom of polyrotaxanes, but their unique architecture leads to rotational, elongational, and torsional degrees of freedom. Polycatenane synthesis requires a ring closing step after macrocyclic complexation and is, therefore, significantly more challenging than polyrotaxane synthesis, limiting the extent of experimental studies.[127,136] Nonetheless, polymerization of catenane precursors has been used to determine, through ultrasonication, that the mechanical bond possesses comparable mechanical strength to purely covalent analogues in linear polymers,[137] suggesting opportunities to probe the potential consequences of conformational flexibility without a cost in ultimate strength within polymer networks.

With covalently linked polymer networks, elasticity at low strains is dominated by the conformational entropy of polymer strands. As the network is stretched, strands within the network increasingly uncoil and the resistance to further uncoiling increases. Eventually, the conformational degrees of freedom decrease to the point that further stretching is dominated by the enthalpic distortion of the strands (i.e., increased bond angles and bond lengths).[138] In SRMs, the initial elasticity is governed by the translational mobility of the sliding crosslinks, and force-coupled displacement is large (Figure 5b). The stiffness of SRMs is, therefore, much lower than a covalently crosslinked material with identical crosslink density (Figure 5c).[139] Once the translational degrees of freedom are exhausted, the effects of traditional network elasticity become important, and there is a characteristic decrease in the force-coupled displacement (Figure 5d).[128] In addition to influencing the stiffness, the translational entropy of the ring has a significant impact on the ultimate properties of SRMs. The sliding of crosslinks in SRMs creates a pulley effect that is believed to redistribute and equalize molecular tension throughout the network (Figure 5e).[132,140] The presumed result is a more homogeneous stress distribution (less broad $p(F)$) in SRMs than in covalently cross-linked networks. Where failure in covalently crosslinked materials can occur at relatively low strains (ca. 100 to 200%)[50] due to inhomogeneous stress distribution, network reorganization allows SRMs to sustain more than 1000% strain without hysteresis.[141]

3.3 Multinetwork elastomers and hydrogels

Lightly crosslinked materials are prized for their extensibility and recovery, but their ability to sustain large deformations comes at the expense of stiffness. At higher crosslink densities and moduli, networks become brittle and more sensitive to defects.[142] In swollen materials, such as hydrogels or organogels, the effects are more pronounced due to the large fraction of solvent and isotropic stretching induced by swelling, and swollen networks typically suffer from poor toughness.[143] To address this dichotomy, Gong and coworkers introduced a novel method to prepare tough hydrogels with hierarchical structure through sequential polymerization and swelling processes (Figure 6).[143] A decade later, Creton and co-workers extended this concept to dry elastomeric networks.[144] The process is simple, yet elegant. A crosslinked network is generated with conventional polymerization techniques, such as free-radical polymerization, using the same monomers and crosslinkers that are common to gels or elastomers. This first network is swollen in a bath of monomer, initiator, and a small amount of crosslinker (much less than used to prepare the first network). Subsequent polymerization forms the second network and traps the first network in an isotropically prestretched state. Additional swelling and polymerization steps are possible from a decrease in the elastic component of the free energy with the introduction of minimally crosslinked networks,[144] where networks 2 through n are collectively referred to as matrix networks. Despite being formed from typically brittle networks, the hierarchical structure in multinetwork materials (MNMs) yields both higher moduli and orders of magnitude increases in fracture toughness over a single network (Figure 7a-c).[143,144]

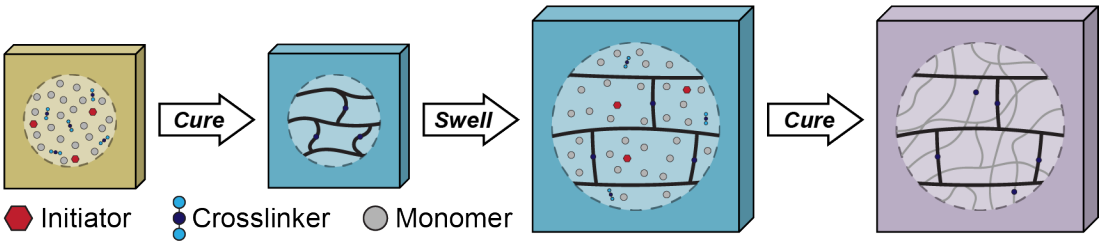

Figure 6. Preparation of multinetwork materials through sequential polymerization and swelling. The first network (black) becomes increasing stretched as it swells during subsequent matrix (gray) preparation steps.

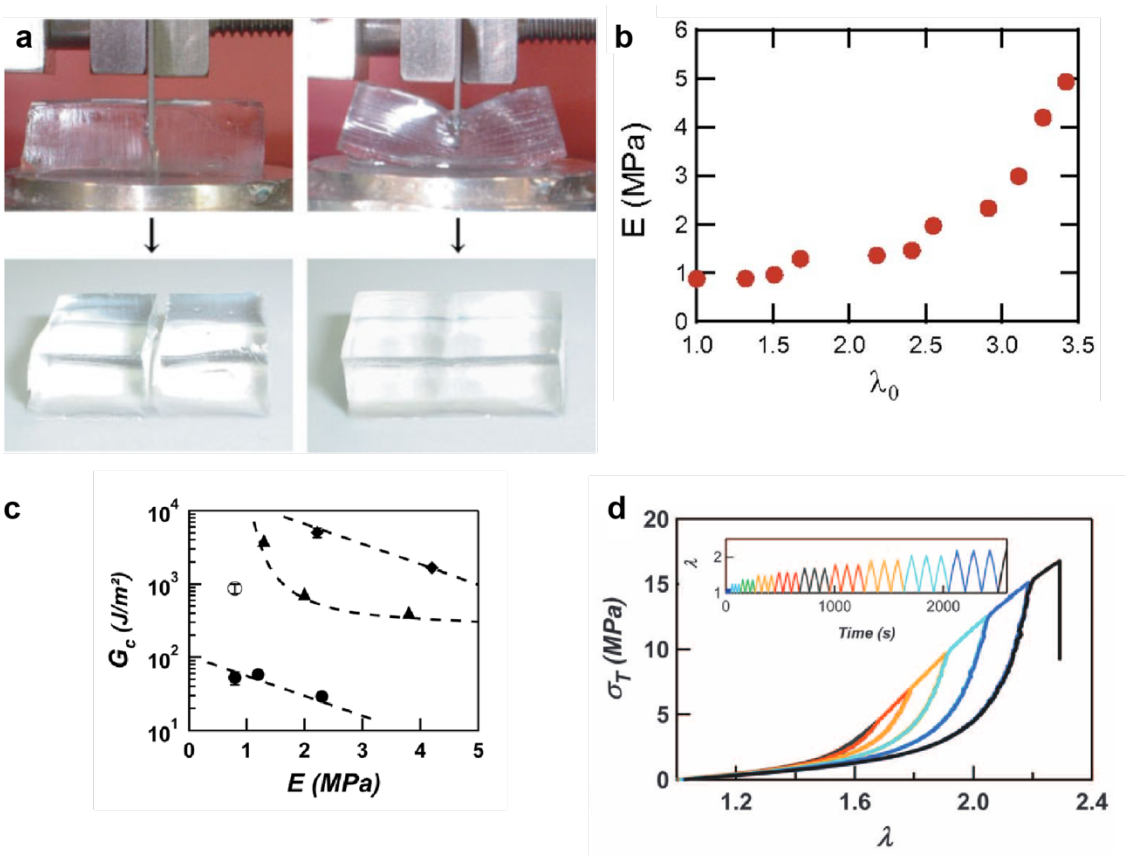

Figure 7. Properties of multinetwork materials. a) Optical images of single network (left) and double network (right) hydrogels subject to slicing with a blade. The extreme toughness of the double network hydrogel resists slicing. b) Young's modulus as a function of the first network prestretch ratio, λ_0. c) Fracture toughness of single network (circles), double network (triangles), and triple network (diamonds) elastomers with varied moduli. d) Stress-strain response of a triple network elastomer subject to cyclic loading. Inset represents the applied stretch versus time. Image (a) reprinted with permission from Ref. 143. Copyright 2003 John Wiley and Sons. Image (b) adapted with permission from Ref. 145. Copyright 2018 Proceedings of National Academy of Sciences. Images (c), (d) from Ref. 144. Reprinted with permission from AAAS.

Creton and coworkers found that the performance of multinetwork elastomers (MNEs) is closely related to the extent of first network prestretch, modulated with the number of swelling and polymerization steps and the amount of solvent introduced during each step (Figure 7b).[145] The more the first network is prestretched, the stiffer and more prone to sacrificial rupture it becomes. As a result, higher order MNEs (i.e. quadruple networks) in which the first network has been repeatedly extended through multiple successive swelling steps, form stable necks when stretched uniaxially; the necking is correlated with the enhanced toughness of the material.[145,146]

The dramatic improvements in fracture toughness are believed to originate in the sacrificial rupture of covalent bonds within the stiff, prestretched first network, while the matrix networks act to transmit load to elastically-active regions of the material.[144–150] Damage accumulation within MNMs was observed during cyclic tensile loading (Figure 7d).[144,145,151] After the first loading cycle, significant softening of the material that increased with maximum applied strain was noted. Negligible hysteresis was observed in subsequent cycles to the same strain, indicating that damage to the network is due to covalent rupture of the filler network. During fracture experiments of double network (DN) hydrogels, Tanaka and coworkers utilized AFM measurements to quantify the extent of softening around a crack tip. They reported an order of magnitude decrease in local Young's modulus when measurements were performed in the undamaged bulk versus directly adjacent to the crack tip.[152] The damage zone was later visualized with a 3D laser microscope and found to extend several hundred microns beyond the crack tip.[153] Covalent rupture has also been monitored at the molecular-level with mechanochemical probes,[144,145,154] which are discussed in the next section. The progressive damage mode that operates during extension or tearing of a hierarchical network allows materials with moduli typically associated with brittle materials to achieve unprecedented strains and energy absorption.

The three classes of contemporary networks explored in this section – topologically controlled networks, mechanically interlocked polymers, and multinetwork materials – present unique and innovative solutions to the challenges of traditional networks. Topological control offers promise in achieving more uniform and narrowly distributed force distributions. Mechanical bonds allow for network reorganization and molecular tension redistribution such that narrow stress distributions are achieved even in an initially heterogeneous network. Finally, efficient energy dissipation mechanisms in MNMs significantly delay the onset of failure in heterogeneous networks, ensuring that a greater number of strands experience high force before fracture.

4. MECHANOCHEMISTRY IN CONTEMPORARY POLYMER NETWORKS

We see great potential synergy at the intersection of polymer mechanochemistry and the types of contemporary polymer network chemistry presented in the preceding section. The abundance of quantified force-coupled responses, including spectroscopic reporters, permits mechanistic, first principles investigations of the molecular states that underlie the complex, macroscopic behavior of polymer networks – in the mathematical terms provided above, using what we know about $G(F)$ to probe how changes in network construction influence $p(F)$ and/or associated behaviors. That molecular understanding will, in turn, inform strategies to improve and optimize network performance. Advances in network chemistry will complement the ongoing design of novel mechanophores by providing platforms that maximize the output of force-coupled responses. In this section, we review recent examples that demonstrate emerging opportunities along these lines. Here, we highlight a few recent examples of mechanochemical coupling in polymer networks, with an emphasis on behaviors related to multi-network materials and slide-ring polymers.

Probing strand tension and scission. Mechanophores have been used in recent years to probe the molecular details of stress and stress transfer in multinetwork elastomers (MNEs), revealing qualitative and quantitative differences relative to conventional single network analogs. Creton and co-workers have employed both dioxetane and spiropyran mechanophores to study the mechanisms behind the unusual properties of these hierarchical materials.[144–146,155,156] In their seminal report, they monitored covalent rupture of the first network with a bis(adamantly)-1,2-dioxetane bisacrylate crosslinker, which emits white light upon scission (Figure 8a-d). Rupture of the dioxetane crosslinker yields an excited-state ketone, and relaxation to the ground state releases a photon of white light. During uniaxial tension, emission (i.e. bond rupture) is only detected beyond a certain stretch ratio, λ, and was homogenously distributed throughout the material. Unloading of the sample and stretching to the same value of λ as the previous cycle resulted in no additional emission, indicating the irreversible rupture of bonds within the first network. Upon further stretching, additional emission was detected, and a direct correlation between the total emission and the mechanical hysteresis was observed. Emission during fracture experiments was found to be distributed in a large region around the crack tip in multinetwork samples but highly localized in single networks. Stress-mapping with a spiropyran mechanophore in MNEs resulted in similar observations.[155] These results support the local damage models for MNMs proposed by Tanaka[157] and Brown,[158] which suggest that the hierarchical structure creates a damage zone that is controlled by the stress to rupture the first network and the transfer of stress between networks. Prior to these studies, the toughening mechanism of MNMs was only validated through macroscopic evidence of bond rupture.[153] In another example of mechanochromophore activation in MNMs, Otsuka and coworkers reported a difluorenylsuccinonitrile (DFSN)-incorporated MNM demonstrated high activation as well as network toughening.[159] Mechanochromic reporting provides clear, molecular-level evidence to support the sacrificial bonding hypothesis and suggests that MNMs hold promise as platforms for enhanced mechanochemical transduction in general.

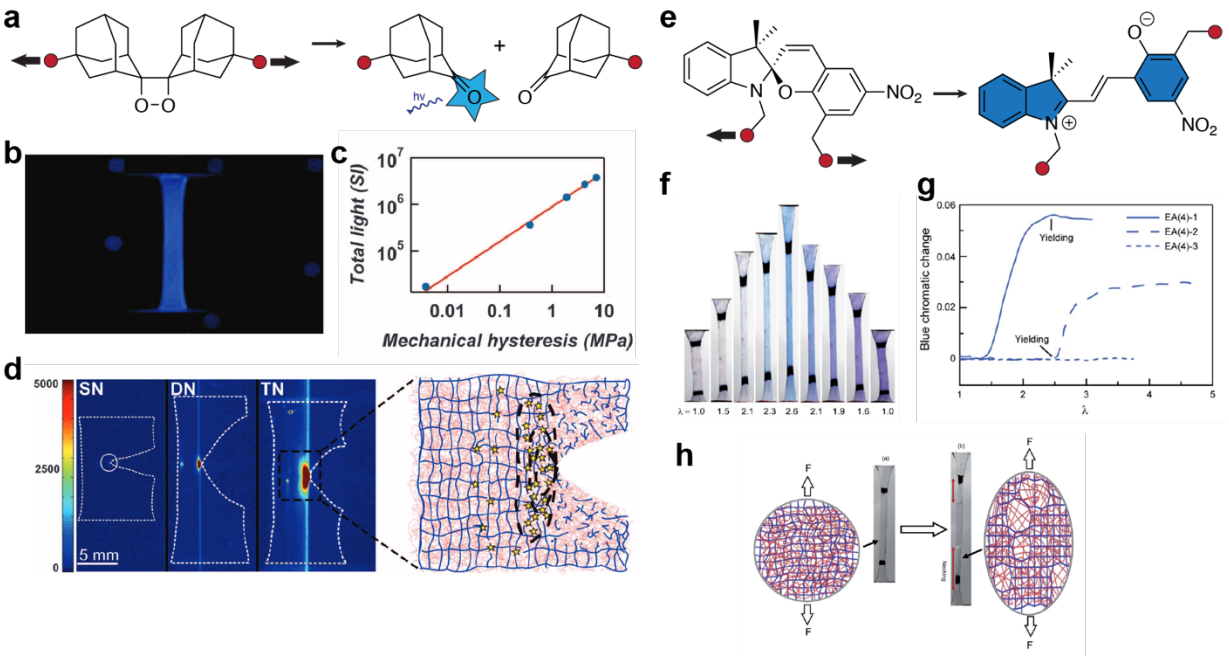

Figure 8. Investigations into the structural features of multinetwork materials enabled by mechanochemistry. a) Mechanoluminescence of 1,2-dioxetane. b) Optical image of triple network with dioxetane crosslinker in the first network under tensile load. c) Total light emission of MNE materials as a function of mechanical hysteresis in cyclic loadings. d) Intensity of luminescence of single, double, and triple network elastomers with dioxetane crosslinker in first network during fracture. e) Mechanochromism of spiropyran. f) Optical images taken at various stages of loading and unloading a multinetwork elastomer with spiropyran. Loading is marked by blue coloration, indicative of spiropyran ring-opening, and unloading is marked a transition to purple, indicative of merocyanine isomerization. g) Chromatic change for quadruple network elastomers with spiropyran embedded in the first, second, or third network. h) Proposed mechanism for damage accumulation in multinetwork elastomers. Image (a-d) from Ref. 144 Reprinted with permission from AAAS. Images (f-h) used with permission of Royal Society of Chemistry, from Mechanochemistry unveils stress transfer during sacrificial bond fracture of tough multiple network elastomers, Chen, Yinjun et al., 12, 2021; permission conveyed through Copyright Clearance Center, Inc.[146]

Transfer of stress between networks is a critical component of the toughness and the stress-strain behavior of MNMs. Models for load transfer were previously set forth based on macroscopic observations.[160,161] The Creton group recently revisited and revised these models with molecular insights provided by spiropyran mechanochromism (Figure 8e).[146] The force-activated conversion of spiropyran to merocyanine is associated with a shift in the absorption spectrum and an observable blue coloration. Upon unloading, the reversion of merocyanine to spiropyran occurs on long time scales, but the rapid isomerization of the unloaded merocyanine results in a second color change from blue to purple (Figure 8f).[156] These chromatic shifts associated with loading and unloading were leveraged to monitor load transfer from the stiff first network to the extensible subsequent networks during necking of MNEs. When spiropyran was incorporated into the first network a chromatic shift from blue to purple was observed instantaneously up neck formation, indicating a partial unloading of the first network strands, and only within the necked region (Figure 8g). The extent of chromatic shift revealed that only 9% of the loaded first network strands were unloaded by covalent rupture upon necking. This observation was inconsistent with the models set forth by Gong and coworkers, which suggested that most of the load was carried by the second network after necking.[160,161] Instead, Creton and coworkers proposed that damage induced by necking results in a local decrease in the crosslink density of the first network, but the first network remains percolated and capable of carrying load (Figure 8h). Further, spiropyran embedded within second network remained inactivated until the onset of necking but continued stretching and propagation of the neck increased the blue coloration, providing definitive proof of load transfer between networks.

Much of the behavior of polymer networks is dominated by relatively low tension behavior of the constituent strands, and so important questions about the interplay of network topology and tension will benefit from probes of low force behavior than are available in covalent mechanophores such as spiropyrans. The molecular reorganization of slide-ring inspired functionalities has recently been used to access these lower tension thresholds at the molecular level. Weder and co-workers have shown that mechanochemically responsive rotaxanes can be easily activated in elastomers by coupling rotaxane translation to the disruption of supramolecular interactions between a luminophore-carrying macrocycle and a

quencher within the axle (Figure 9).[28,162,163] The low force, supramolecular mechanochromism was observed at lower stresses and strains and much higher ultimate levels of activation (up to 29%) than is typical of covalent mechanophores like spiropyran, and it is rapidly reversible and repeatable over at least twenty loading-unloading cycles.[162] Further, dual function mechanophores were demonstrated by controlling the size of the stopper on the rotaxane axle.[28] The reversible mechanochromism was retained at low forces, but at higher stress/strain the use of smaller stoppers led to irreversible luminescence that was attributed to the dethreading of the mechanical bond, providing opportunities for ratiometric measures of different force thresholds in a network. [162]

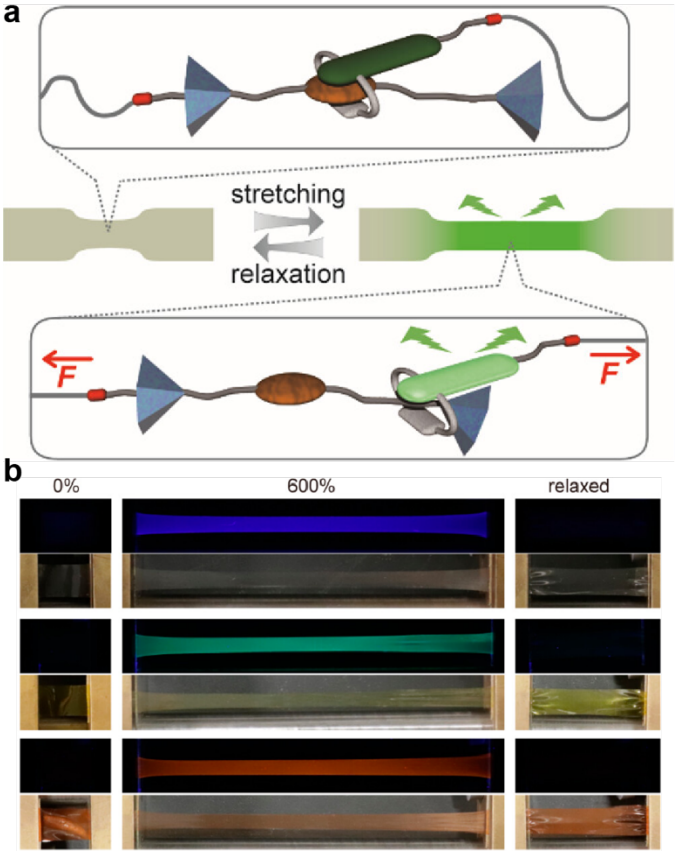

Figure 9. Mechanophore activation in slide-ring materials. a) Schematic representation of slide ring-mechanophore. Charge transfer interactions between macrocyclic ring and quencher within the rotaxane axle suppresses luminescence. Translation of rotaxane when subject to force disrupts interaction and luminescence revealed. b) Optical and fluorescent images of three different rotaxane mechanophores upon stretching and relaxing. Image (a) adapted with permission from Ref. 162. Copyright 2018 American Chemical Society. Image (b) reproduced with permission from Ref. 163. Copyright 2019 American Chemical Society.

The nature of the network design can have a significant impact on the extent of mechanophore activation that can be achieved, relative to the modest values (often less than 1%) in simple networks. DFSN[159] and RSE[101] mechanophores embedded in multinetwork materials are reported to undergo 1 – 1.5% activation under uniaxial strain, and luminophores in MIPS[162] roughly 29%. The method by which force is applied results in notable differences in activation values. A gated mechanoacid with activation forces of approximately 2 nN obtained activation levels of 0.8% under quasi-static uniaxial strain, and repeated hammer strikes brought that to 1.7%.[164] Even outside of MNMs and MIPs, the way in which polymer topology channels force to specific molecular components has important consequences for polymer fracture. Otsuka has extensively studied the focusing effect of well-defined branched architectures to direct applied force to centralized mechanophores in the bulk.[165–167] For example, star polymers enhance force transmission to centrally placed, scissile DABBF mechanophores.[165] When ground, powders of two-arm (linear) polymers led to 14% DABBF scission, while four-arm and eight-arm polymers led to 26% and 46% scission, respectively. An increase of up to23-fold was observed in the response of DABBF-centered dendrimers by grinding, which increases with dendrimer generation.[166] The topological gradients (from edge to center) that are intrinsic to star and dendritic architectures suggest opportunities for focusing macroscopic tension to the core of these structures in elastomeric networks. The range of activation methods and assessments in the above examples highlight that strategies to improve mechanophore activation will depend on context, for example whether activation prior to material failure or activation at a given material stress or strain is the goal.

Recently, some of us explored the connection between the strength of a scissile mechanophore and the toughness of polymer gels (Figure 10).[115] Azide-terminated tetra-arm poly(ethylene glycol) precursors were end-linked with bis-alkyne terminated mechanophores through copper(I)-catalyzed azide-alkyne cycloaddition to form gels with indistinguishable moduli and swelling behavior. The structural homology of the gels allowed us to focus solely on the connection between molecular and macroscopic behavior. Force-coupled reactivity of mechanophore linkers determines the toughness of polymer gels: gels with relatively weak scissile linkers possessed tearing energies of 3 J m^{-2} while those with strong linkers exhibited a nearly 10-fold increase in tearing energy. Although not yet applied in this context, this approach is well suited for future systematic studies of how network topology, controlled and characterized using techniques described in Section 3.1, influences mechanochemical transduction.

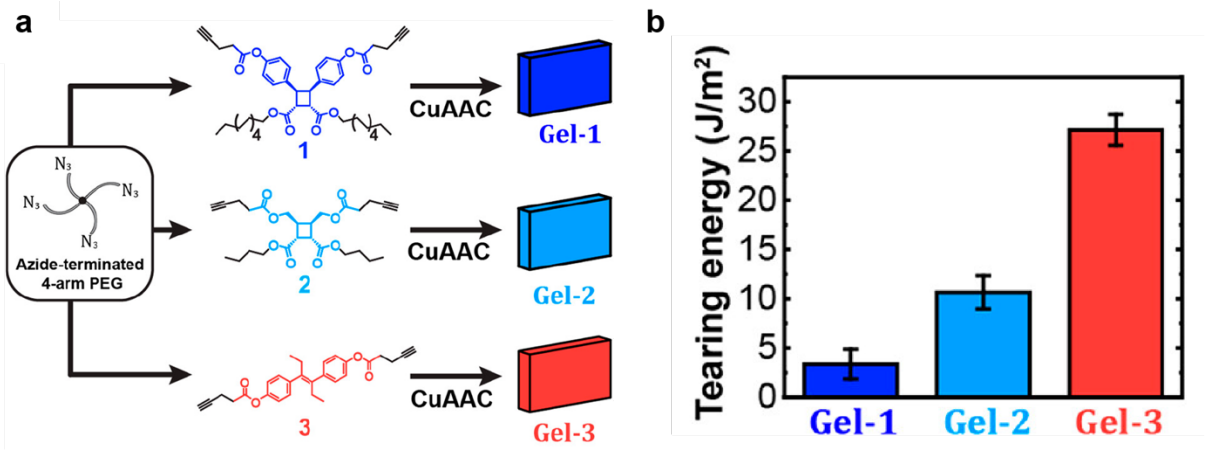

Figure 10. Molecular investigation of network properties through mechanochemistry. a) End-linking of an azide-terminated four-arm PEG precursor with bifunctional linkers containing mechanophores with varied breaking strengths. b) Tearing energies of the three gels. Images (a), (b) adapted with permission from Ref. 115. Copyright 2021 American Chemical Society.

Scissile mechanophores might also play an important role in validating the translational and rotational freedoms offered by MIPs, complementing the work of Weder described above. Zhang and De Bo studied the slide-ring behavior of rotaxanes with a mechanically-labile Diels-Alder adduct incorporated at one end of the rotaxane axle.[168] The presence of a mechanical bond decreases mechanochemical activity during solution-state ultrasonication. Computational models suggest that tension first drives the rotaxane macrocycle to the end of the chain, where it encounters the stopper and stress is subsequently diverted to the mechanical bond. Lu and coworkers extended this work to slide-ring networks by embedding diarylbibenzofuranone (DABBF) mechanophores into rotaxane crosslinks.[169] They observed a delay in the onset of DABBF dissociation compared to covalently bound networks, consistent with reorganization of the network and redistribution of stress through rotaxane translation. Similarly, rotation of catenated rings helps to redistribute tension in a catenated network, delaying the onset of mechanophore activation and covalent bond rupture until a more uniform force distribution is achieved.[27]

Mechanochemical enhancements to network properties. The structural features of hierarchical networks have been shown to improve mechanophore activation.[170,171] When mechanophores are embedded into the first network of an MNM, the isotropic prestretching of the first network during subsequent network formation overcomes a large portion of first network's entropic elasticity. Subsequently, the strain required to begin deforming the mechanophore is much lower. Qiu and coworkers reported critical activation strains for spiropyran containing MNEs as low as 40%,[170] less than half of the critical activation strain reported in conventional PDMS elastomers.[50,52] Similarly, Wang and coworkers observed critical activation strains of 150% for rhodamine functionalized double network (DN) hydrogels[171] vs. more than 300% strain in single network hydrogels.[172] Further the energy dissipation and load transfer mechanisms operative during loading ensure high strain to failure and activation of a greater proportion of embedded mechanophores. MNEs prepared by Qiu and coworkers survived up to 700% strain, resulting for the first time in mechanochromic spiropyran activation that is greater than photochromic activation.[170]

Aside from improving mechanophore activation, we and several other groups have harnessed and reinforced the unique features of hierarchical networks to further improve their properties. Boulatov, Creton, and Weng utilized a photochemically repairable mechanophore to heal and remodel MNEs after sacrificial rupture of the first network.[173] Dissociation of anthracene dimer crosslinks upon loading revealed highly fluorescent anthracenes that could be recombined via irradiation with UV-light. Interestingly, irradiation of the damaged networks resulted in network

reorganization where some pendant anthracenes reformed crosslinks while others formed elastically inactive loops. The remodeled MNEs retained 70% of their original energy dissipation capacity even after three loading and irradiation cycles. Inspired by muscle growth through repetitive loading, Gong and co-workers leveraged the mechanoradicals generated during sacrificial network rupture to initiate polymerization within DN hydrogels (Figure 11 a,b).[6] They found that the concentration of radicals was directly linked to the extent of covalent bond rupture within the first network. Further, when extension was performed in a bath of monomer and crosslinker, the generated radicals polymerized the absorbed reactants into a new network. Monomer conversion was found to be as high as 90%, and cyclic loading and unloading within a reactant bath led to the growth and strengthening of the original double network. More recently, Gong's group also reported an azoalkane-crosslinked DN hydrogel for more efficient mechanoradicals generation amplified by a factor of 5 compared to a traditional acrylamide-based crosslinker.[174] While new bond generation by mechanoradicals has been observed previously in polybutadienes and other materials,[175–177] the ability to recover initial shape and feed growth through monomer addition offers distinct advantages to the MNE strategy. [174–176]In a recent publication, we showed that the toughness of DN hydrogels is influenced by incorporating reactive strand extension (RSE) mechanophores into the backbone of the sacrificial network (Figure 11c-e).[101] RSE mechanophores release stored length and extend the polymer backbone upon activation, providing molecular stress relief. Since activation occurs close to the breaking point of polymer chains, remodeling of the polymer network dissipates significantly more energy than in strands that are programmed to break at the point of RSE onset. As a result, RSE doubled the strain at failure and the tearing energy over control DN hydrogels.

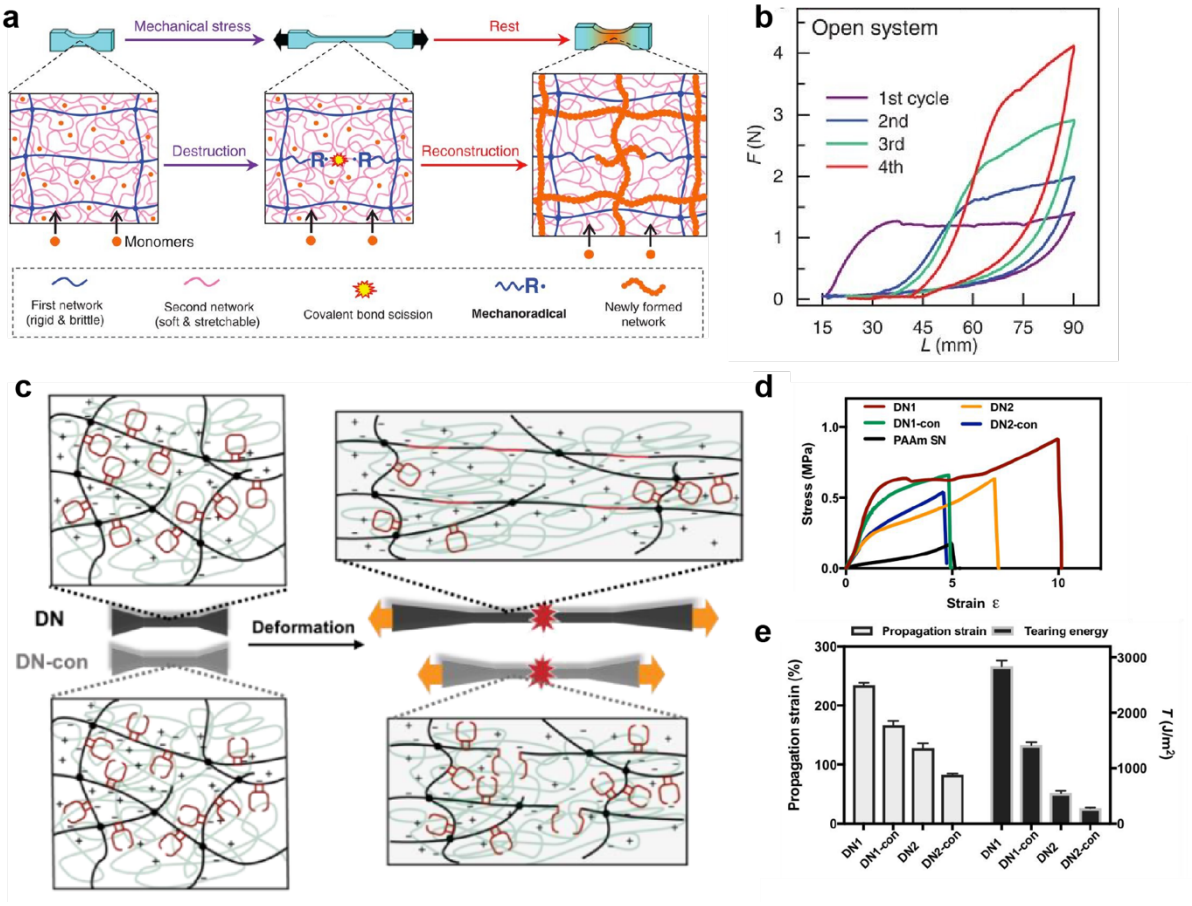

Figure 11. Reinforcing hierarchical structure with mechanochemistry. a) Schematic representation double network hydrogel growth and strengthening through mechanoradical generation and subsequent polymerization. b) Stress-strain response of double network hydrogels loaded within a bath of monomer and crosslinker. c) Concept of reactive strand extension within double network hydrogels. d) Stress-strain response for various hydrogels under tensile deformation. e) Critical strain for crack propagation and tearing energy of double network hydrogels with and without RSE. Images (a), (b) from Ref. 6. Reprinted with permission from AAAS. Images (c–e) from Ref. 101. Reprinted with permission from AAAS.

5. FUTURE PERSPECTIVES AND OUTLOOKS

Recent advances in polymer network chemistry have enabled the synthesis and characterization of networks with relatively well-defined topologies and hierarchical structure. Those topologies have implications both for the molecular scale distribution of tension within the network and the macroscopic limits of mechanical performance of the network. Polymer mechanochemistry holds the potential to link behavior at these two scales. Its combination with contemporary polymer network chemistry has already led to several molecular-level descriptions of network behavior, significant improvements in mechanochemical transduction, and complementary enhancements of network performance. Looking ahead, the marriage of these two active areas of research is expected to create synergies that amplify the advancements of the respective fields.

Over the next decade, we envision that mechanophores will be utilized to harness and reinforce the unique structural features of hierarchical networks. Strategies like reactive strand extension[101] or mechanically induced growth[6] have shown great promise in improving the performance of these already advanced materials, and we expect that similar mechanochemical strategies will bring novel functions to MNMs. Further, we are excited by the potential to extend mechanically active slide-ring materials to molecular responses other than luminescence. The molecular rearrangement of MIPs enables large changes in force-coupled distance, and we therefore predict very large changes in chemical potential at relatively low forces and unprecedented force-coupled reactivity. We also see excellent opportunities to combine advances in topological control with hierarchical networks. Early investigations indicate that the performance of MNMs can be improved with more homogeneous first networks.[178] These advances in function will be accompanied, and often driven, by the use of mechanophores as molecular probes. Quantified molecular responses will provide answers to molecular-level questions about the underlying physics and structure-activity relationships of contemporary network architectures and how they differ from conventional networks. We can then use newly acquired network information to improve both network and mechanophore design.

Looking even further, we see opportunities at another level of material topology, namely that found in architected (meta)materials. Polymer mechanochemistry will be further enhanced by designing material structure on multiple length scales, from the (macro)molecular level to the macroscopic structure. In particular, the stimuli-induced macroscopic reorganization of bistable structures[179,180] highlight how small external stimuli lead to massive changes in geometry. We suspect that coupling polymer mechanochemistry with mechanical metamaterials will lead to signal amplification cascades that capitalize more fully on the chemical potential of mechanophores. Whether there are direct and meaningful connections that might be drawn between topology at the molecular/network level (where thermal fluctuations contribute to behavior) and that at the metamaterial level (where thermal fluctuations do not contribute) to guide predictive design on either/both length scales feels like a timely, if enormously speculative, question that is well suited to a favorite bar or coffee house. We look forward to those conversations.

Author Information

Corresponding Author

Stephen L. Craig – NSF Center for the Chemistry of Molecularly Optimized Networks and Department of Chemistry, Duke University, Durham, North Carolina, 27708, United States; Email: stephen.craig@duke.edu

Authors

Evan M. Lloyd – Department of Chemistry, Duke University, Durham, North Carolina, 27708, United States

Jafer R. Vakil – NSF Center for the Chemistry of Molecularly Optimized Networks and Department of Chemistry, Duke University, Durham, North Carolina, 27708, United States

Yunxin Yao – NSF Center for the Chemistry of Molecularly Optimized Networks and Department of Chemistry, Duke University, Durham, North Carolina, 27708, United States

Nancy Sottos – NSF Center for the Chemistry of Molecularly Optimized Networks, Duke University, Durham, NC 27708, United States; Materials Science and Engineering, University of Illinois Urbana-Champaign, Urbana, Illinois 61801, United States.

ACKNOWLEDGEMENTS

This work was supported by the NSF Center for the Chemistry of Molecularly Optimized Networks (MONET), CHE-2116298, and Duke University.

References:

(1) Davis, D. A.; Hamilton, A.; Yang, J.; Cremar, L. D.; Gough, D. V.; Potisek, S. L.; Ong, M. T.; Braun, P. V.; Martínez, T. J.; White, S. R.; Moore, J. S.; Sottos, N. R. Force-Induced Activation of Covalent Bonds in Mechanoresponsive Polymeric Materials. *Nature* **2009**, *459* (7243), 68 72. https://doi.org/10.1038/nature07970.

(2) Kean, Z. S.; Craig, S. L. Mechanochemical Remodeling of Synthetic Polymers. *Polymer* **2012**, *53* (5), 1035 1048. https://doi.org/10.1016/j.polymer.2012.01.018.

(3) Gossweiler, G. R.; Brown, C. L.; Hewage, G. B.; Sapiro-Gheiler, E.; Trautman, W. J.; Welshofer, G. W.; Craig, S. L. Mechanochemically Active Soft Robots. *Acs Appl Mater Inter* **2015**, *7* (40), 22431–22435. https://doi.org/10.1021/acsami.5b06440.

(4) Chen, Z.; Mercer, J. A. M.; Zhu, X.; Romaniuk, J. A. H.; Pfattner, R.; Cegelski, L.; Martinez, T. J.; Burns, N. Z.; Xia, Y. Mechanochemical Unzipping of Insulating Polyladderene to Semiconducting Polyacetylene. *Science* **2017**, *357* (6350), 475–479. https://doi.org/10.1126/science.aan2797.

(5) Zhang, H.; Gao, F.; Cao, X.; Li, Y.; Xu, Y.; Weng, W.; Boulatov, R. Mechanochromism and Mechanical-Force-Triggered Cross-Linking from a Single Reactive Moiety Incorporated into Polymer Chains. *Angewandte Chemie Int Ed* **2016**, *55* (9), 3040 3044. https://doi.org/10.1002/anie.201510171.

(6) Matsuda, T.; Kawakami, R.; Namba, R.; Nakajima, T.; Gong, J. P. Mechanoresponsive Self-Growing Hydrogels Inspired by Muscle Training. *Science* **2019**, *363* (6426), 504–508. https://doi.org/10.1126/science.aau9533.

(7) Lenhardt, J. M.; Ong, M. T.; Choe, R.; Evenhuis, C. R.; Martinez, T. J.; Craig, S. L. Trapping a Diradical Transition State by Mechanochemical Polymer Extension. *Science* **2010**, *329* (5995), 1057–1060. https://doi.org/10.1126/science.1193412.

(8) Hickenboth, C. R.; Moore, J. S.; White, S. R.; Sottos, N. R.; Baudry, J.; Wilson, S. R. Biasing Reaction Pathways with Mechanical Force. *Nature* **2007**, *446* (7134), 423-427. https://doi.org/10.1038/nature05681.

(9) Chen, Z.; Zhu, X.; Yang, J.; Mercer, J. A. M.; Burns, N. Z.; Martinez, T. J.; Xia, Y. The Cascade Unzipping of Ladderane Reveals Dynamic Effects in Mechanochemistry. *Nat Chem* **2020**, *12*, 302-209. https://doi.org/10.1038/s41557-019-0396-5.

(10) Liu, Y.; Holm, S.; Meisner, J.; Jia, Y.; Wu, Q.; Woods, T. J.; Martinez, T. J.; Moore, J. S. Flyby Reaction Trajectories: Chemical Dynamics under Extrinsic Force. *Science* **2021**, *373* (6551), 208–212. https://doi.org/10.1126/science.abi7609.

(11) Berkowski, K. L.; Potisek, S. L.; Hickenboth, C. R.; Moore, J. S. Ultrasound-Induced Site-Specific Cleavage of Azo-Functionalized Poly(Ethylene Glycol). *Macromolecules* **2005**, *38* (22), 8975 8978. https://doi.org/10.1021/ma051394n.

(12) Verstraeten, F.; Göstl, R.; Sijbesma, R. P. Stress-Induced Colouration and Crosslinking of Polymeric Materials by Mechanochemical Formation of Triphenylimidazolyl Radicals. *Chem Commun* **2016**, *52* (55), 8608–8611. https://doi.org/10.1039/c6cc04312g.

(13) Imato, K.; Irie, A.; Kosuge, T.; Ohishi, T.; Nishihara, M.; Takahara, A.; Otsuka, H. Mechanophores with a Reversible Radical System and Freezing-Induced Mechanochemistry in Polymer Solutions and Gels. *Angew Chem-ger Edit* **2015**, *127* (21), 6266–6270. https://doi.org/10.1002/ange.201412413.

(14) Larsen, M. B.; Boydston, A. J. Successive Mechanochemical Activation and Small Molecule Release in an Elastomeric Material. *J Am Chem Soc* **2014**, *136* (4), 1276–1279. https://doi.org/10.1021/ja411891x.

(15) Lin, Y.; Kouznetsova, T. B.; Craig, S. L. A Latent Mechanoacid for Time-Stamped Mechanochromism and Chemical Signaling in Polymeric Materials. *J Am Chem Soc* **2020**, *142* (1), 99-103. https://doi.org/10.1021/jacs.9b12861.

(16) Hu, X.; Zeng, T.; Husic, C. C.; Robb, M. J. Mechanically Triggered Small Molecule Release from a Masked Furfuryl Carbonate. *J Am Chem Soc* **2019**, *141* (38), 15018–15023. https://doi.org/10.1021/jacs.9b08663.

(17) Zhang, Y.; Wang, Z.; Kouznetsova, T. B.; Sha, Y.; Xu, E.; Shannahan, L.; Fermen-Coker, M.; Lin, Y.; Tang, C.; Craig, S. L. Distal Conformational Locks on Ferrocene Mechanophores Guide Reaction Pathways for Increased Mechanochemical Reactivity. *Nat Chem* **2021**, *13* (1), 56–62. https://doi.org/10.1038/s41557-020-00600-2.

(18) Hu, X.; Zeng, T.; Husic, C. C.; Robb, M. J. Mechanically Triggered Release of Functionally Diverse Molecular Payloads from Masked 2-Furylcarbinol Derivatives. *Acs Central Sci* **2021,** *7* (7), 1216–1224. https://doi.org/10.1021/acscentsci.1c00460.

(19) Giannantonio, M. D.; Ayer, M. A.; Verde-Sesto, E.; Lattuada, M.; Weder, C.; Fromm, K. M. Triggered Metal Ion Release and Oxidation: Ferrocene as a Mechanophore in Polymers. *Angewandte Chemie Int Ed* **2018**, *57* (35), 11445–11450. https://doi.org/10.1002/anie.201803524.

(20) Shen, H.; Larsen, M. B.; Roessler, A.; Zimmerman, P.; Boydston, A. J. Mechanochemical Release of N-heterocyclic Carbenes from Flex-Activated Mechanophores. *Angewandte Chemie Int Ed* **2021,** *60* (24), 13559-13563. https://doi.org/10.1002/anie.202100576.

(21) Shi, Z.; Song, Q.; Göstl, R.; Herrmann, A. Mechanochemical Activation of Disulfide-Based Multifunctional Polymers for Theranostic Drug Release. *Chem Sci* **2020**, *12* (5), 1668–1674. https://doi.org/10.1039/d0sc06054b.

(22) Wu, D.; Lenhardt, J. M.; Black, A. L.; Akhremitchev, B. B.; Craig, S. L. Molecular Stress Relief through a Force-Induced Irreversible Extension in Polymer Contour Length. *J Am Chem Soc* **2010**, *132* (45), 15936–15938. https://doi.org/10.1021/ja108429h.

(23) Kean, Z. S.; Niu, Z.; Hewage, G. B.; Rheingold, A. L.; Craig, S. L. Stress-Responsive Polymers Containing Cyclobutane Core Mechanophores: Reactivity and Mechanistic Insights. *J Am Chem Soc* **2013**, *135* (36), 13598–13604. https://doi.org/10.1021/ja4075997.

(24) Wang, J.; Kouznetsova, T. B.; Boulatov, R.; Craig, S. L. Mechanical Gating of a Mechanochemical Reaction Cascade. *Nat Commun* **2016**, *7* (1), 13433. https://doi.org/10.1038/ncomms13433.

(25) Bowser, B. H.; Ho, C.-H.; Craig, S. L. High Mechanophore Content, Stress-Relieving Copolymers Synthesized via RAFT Polymerization. *Macromolecules* **2019**, *52* (22), 9032–9038. https://doi.org/10.1021/acs.macromol.9b01792.

(26) Tian, Y.; Cao, X.; Li, X.; Zhang, H.; Sun, C.-L.; Xu, Y.; Weng, W.; Zhang, W.; Boulatov, R. A Polymer with Mechanochemically Active Hidden Length. *J Am Chem Soc* **2020**, *142* (43), 18687–18697. https://doi.org/10.1021/jacs.0c09220.

(27) Zhang, M.; Bo, G. D. A Catenane as a Mechanical Protecting Group. *J Am Chem Soc* **2020**, *142* (11), 5029–5033. https://doi.org/10.1021/jacs.0c01757.

(28) Muramatsu, T.; Okado, Y.; Traeger, H.; Schrettl, S.; Tamaoki, N.; Weder, C.; Sagara, Y. Rotaxane-Based Dual Function Mechanophores Exhibiting Reversible and Irreversible Responses. *J Am Chem Soc* **2021,** *143* (26), 9884–9892. https://doi.org/10.1021/jacs.1c03790.

(29) Imato, K.; Irie, A.; Kosuge, T.; Ohishi, T.; Nishihara, M.; Takahara, A.; Otsuka, H. Mechanophores with a Reversible Radical System and Freezing-Induced Mechanochemistry in Polymer Solutions and Gels. *Angewandte Chemie Int Ed* **2015**, *54* (21), 6168–6172. https://doi.org/10.1002/anie.201412413.

(30) McFadden, M. E.; Robb, M. J. Generation of an Elusive Permanent Merocyanine via a Unique Mechanochemical Reaction Pathway. *J Am Chem Soc* **2021**, *143* (21), 7925–7929. https://doi.org/10.1021/jacs.1c03865.

(31) Zhang, H.; Gao, F.; Cao, X.; Li, Y.; Xu, Y.; Weng, W.; Boulatov, R. Mechanochromism and Mechanical-Force-Triggered Cross-Linking from a Single Reactive Moiety Incorporated into Polymer Chains. *Angewandte Chemie Int Ed* **2016**, *55* (9), 3040–3044. https://doi.org/10.1002/anie.201510171.

(32) Robb, M. J.; Kim, T. A.; Halmes, A. J.; White, S. R.; Sottos, N. R.; Moore, J. S. Regioisomer-Specific Mechanochromism of Naphthopyran in Polymeric Materials. *J Am Chem Soc* **2016**, *138* (38), 12328–12331. https://doi.org/10.1021/jacs.6b07610.

(33) Sumi, T.; Goseki, R.; Otsuka, H. Tetraarylsuccinonitriles as Mechanochromophores to Generate Highly Stable Luminescent Carbon-Centered Radicals. *Chem Commun* **2017**, *53* (87), 11885–11888. https://doi.org/10.1039/c7cc06913h.

(34) Qian, H.; Purwanto, N. S.; Ivanoff, D. G.; Halmes, A. J.; Sottos, N. R.; Moore, J. S. Fast, Reversible Mechanochromism of Regioisomeric Oxazine Mechanophores: Developing in Situ Responsive Force Probes for Polymeric Materials. *Chem* **2021**, *7* (4), 1080–1091. https://doi.org/10.1016/j.chempr.2021.02.014.

(35) Yamakado, T.; Saito, S. Ratiometric Flapping Force Probe That Works in Polymer Gels. *J Am Chem Soc* **2022**, *144* (6), 2804–2815. https://doi.org/10.1021/jacs.1c12955.

(36) Piermattei, A.; Karthikeyan, S.; Sijbesma, R. P. Activating Catalysts with Mechanical Force. *Nat Chem* **2009**, *1* (2), 133 137. https://doi.org/10.1038/nchem.167.

(37) Jakobs, R. T. M.; Sijbesma, R. P. Mechanical Activation of a Latent Olefin Metathesis Catalyst and Persistence of Its Active Species in ROMP. *Organometallics* **2012**, *31* (6), 2476 2481. https://doi.org/10.1021/om300161z.

(38) Michael, P.; Binder, W. H. A Mechanochemically Triggered "Click" Catalyst. *Angewandte Chemie Int Ed* **2015**, *54* (47), 13918–13922. https://doi.org/10.1002/anie.201505678.

(39) Lenhardt, J. M.; Black, A. L.; Craig, S. L. Gem -Dichlorocyclopropanes as Abundant and Efficient Mechanophores in Polybutadiene Copolymers under Mechanical Stress. *J Am Chem Soc* **2009**, *131* (31), 10818–10819. https://doi.org/10.1021/ja9036548.

(40) Schwartz, J. J.; Behrou, R.; Cao, B.; Bassford, M.; Mendible, A.; Shaeffer, C.; Boydston, A. J.; Boechler, N. Reduced Strain Mechanochemical Activation Onset in Microstructured Materials. *Polym Chem-uk* **2020**, *11* (6), 1122–1126. https://doi.org/10.1039/c9py01875a.

(41) Chen, Y.; Mellot, G.; Luijk, D. van; Creton, C.; Sijbesma, R. P. Mechanochemical Tools for Polymer Materials. *Chem Soc Rev* **2021,** *50* (6), 4100–4140. https://doi.org/10.1039/d0cs00940g.

(42) Li, J.; Nagamani, C.; Moore, J. S. Polymer Mechanochemistry: From Destructive to Productive. *Accounts Chem Res* **2015**, *48* (8), 2181-2190. https://doi.org/10.1021/acs.accounts.5b00184.

(43) Willis-Fox, N.; Rognin, E.; Aljohani, T. A.; Daly, R. Polymer Mechanochemistry: Manufacturing Is Now a Force to Be Reckoned With. *Chem* **2018**, *4* (11), 2499–2537. https://doi.org/10.1016/j.chempr.2018.08.001.

(44) Ghanem, M. A.; Basu, A.; Behrou, R.; Boechler, N.; Boydston, A. J.; Craig, S. L.; Lin, Y.; Lynde, B. E.; Nelson, A.; Shen, H.; Storti, D. W. The Role of Polymer Mechanochemistry in Responsive Materials and Additive Manufacturing. *Nat Rev Mater* **2020**, *6*, 84-98. https://doi.org/10.1038/s41578-020-00249-w.

(45) O'Neill, R. T.; Boulatov, R. The Many Flavours of Mechanochemistry and Its Plausible Conceptual Underpinnings. *Nat Rev Chem* **2021**, *5*, 148-167. https://doi.org/10.1038/s41570-020-00249-y.

(46) Kersey, F. R.; Yount, W. C.; Craig, S. L. Single-Molecule Force Spectroscopy of Bimolecular Reactions: System Homology in the Mechanical Activation of Ligand Substitution Reactions. *J Am Chem Soc* **2006**, *128* (12), 3886–3887. https://doi.org/10.1021/ja058516b.

(47) Lenhardt, J. M.; Black, A. L.; Beiermann, B. A.; Steinberg, B. D.; Rahman, F.; Samborski, T.; Elsakr, J.; Moore, J. S.; Sottos, N. R.; Craig, S. L. Characterizing the Mechanochemically Active Domains in Gem -Dihalocyclopropanated Polybutadiene under Compression and Tension. *J Mater Chem* **2011**, *21* (23), 8454–8459. https://doi.org/10.1039/c0jm04117c.

(48) Gossweiler, G. R.; Hewage, G. B.; Soriano, G.; Wang, Q.; Welshofer, G. W.; Zhao, X.; Craig, S. L. Mechanochemical Activation of Covalent Bonds in Polymers with Full and Repeatable Macroscopic Shape Recovery. *Acs Macro Lett* **2014**, *3* (3), 216 219. https://doi.org/10.1021/mz500031q.

(49) Robb, M. J.; Kim, T. A.; Halmes, A. J.; White, S. R.; Sottos, N. R.; Moore, J. S. Regioisomer-Specific Mechanochromism of Naphthopyran in Polymeric Materials. *J Am Chem Soc* **2016**, *138* (38), 12328–12331. https://doi.org/10.1021/jacs.6b07610.

(50) Lin, Y.; Barbee, M. H.; Chang, C.-C.; Craig, S. L. Regiochemical Effects on Mechanophore Activation in Bulk Materials. *J Am Chem Soc* **2018**, *140* (46), 15969–15975. https://doi.org/10.1021/jacs.8b10376.

(51) Sha, Y.; Zhang, Y.; Xu, E.; Wang, Z.; Zhu, T.; Craig, S. L.; Tang, C. Quantitative and Mechanistic Mechanochemistry in Ferrocene Dissociation. *Acs Macro Lett* **2018**, *7* (10), 1174–1179. https://doi.org/10.1021/acsmacrolett.8b00625.

(52) Kim, T. A.; Robb, M. J.; Moore, J. S.; White, S. R.; Sottos, N. R. Mechanical Reactivity of Two Different Spiropyran Mechanophores in Polydimethylsiloxane. *Macromolecules* **2018**, *51* (22), 9177–9183. https://doi.org/10.1021/acs.macromol.8b01919.

(53) Kim, T. A.; Lamuta, C.; Kim, H.; Leal, C.; Sottos, N. R. Interfacial Force-Focusing Effect in Mechanophore-Linked Nanocomposites. *Adv Sci* **2020**, *7* (7), 1903464. https://doi.org/10.1002/advs.201903464.

(54) Beiermann, B. A.; Kramer, S. L. B.; May, P. A.; Moore, J. S.; White, S. R.; Sottos, N. R. The Effect of Polymer Chain Alignment and Relaxation on Force-Induced Chemical Reactions in an Elastomer. *Adv Funct Mater* **2014**, *24* (11), 1529–1537. https://doi.org/10.1002/adfm.201302341.

(55) Beiermann, B. A.; Kramer, S. L. B.; Moore, J. S.; White, S. R.; Sottos, N. R. Role of Mechanophore Orientation in Mechanochemical Reactions. *Acs Macro Lett* **2012**, *1* (1), 163–166. https://doi.org/10.1021/mz2000847.

(56) Fang, X.; Zhang, H.; Chen, Y.; Lin, Y.; Xu, Y.; Weng, W. Biomimetic Modular Polymer with Tough and Stress Sensing Properties. *Macromolecules* **2013**, *46* (16), 6566–6574. https://doi.org/10.1021/ma4014862.

(57) Chen, Y.; Zhang, H.; Fang, X.; Lin, Y.; Xu, Y.; Weng, W. Mechanical Activation of Mechanophore Enhanced by Strong Hydrogen Bonding Interactions. *Acs Macro Lett* **2014**, *3* (2), 141–145. https://doi.org/10.1021/mz400600r.

(58) Lenhardt, J. M.; Ramirez, A. L. B.; Lee, B.; Kouznetsova, T. B.; Craig, S. L. Mechanistic Insights into the Sonochemical Activation of Multimechanophore Cyclopropanated Polybutadiene Polymers. *Macromolecules* **2015**, *48* (18), 6396–6403. https://doi.org/10.1021/acs.macromol.5b01677.

(59) Lin, Y.; Kouznetsova, T. B.; Craig, S. L. Mechanically Gated Degradable Polymers. *J Am Chem Soc* **2020,** *142* (5), 2105–2109. https://doi.org/10.1021/jacs.9b13359.

(60) Sun, Y.; Neary, W. J.; Burke, Z. P.; Qian, H.; Zhu, L.; Moore, J. S. Mechanically Triggered Carbon Monoxide Release with Turn-On Aggregation-Induced Emission. *J Am Chem Soc* **2022**, *144* (3), 1125–1129. https://doi.org/10.1021/jacs.1c12108.

(61) Bowser, B. H.; Craig, S. L. Empowering Mechanochemistry with Multi-Mechanophore Polymer Architectures. *Polym Chem-uk* **2018**, *9* (26), 3583–3593. https://doi.org/10.1039/c8py00720a.

(62) Klukovich, H. M.; Kouznetsova, T. B.; Kean, Z. S.; Lenhardt, J. M.; Craig, S. L. A Backbone Lever-Arm Effect Enhances Polymer Mechanochemistry. *Nat Chem* **2013**, *5* (2), 110–114. https://doi.org/10.1038/nchem.1540.

(63) Bowser, B. H.; Wang, S.; Kouznetsova, T. B.; Beech, H. K.; Olsen, B. D.; Rubinstein, M.; Craig, S. L. Single-Event Spectroscopy and Unravelling Kinetics of Covalent Domains Based on Cyclobutane Mechanophores. *J Am Chem Soc* **2021**, *143* (13), 5269–5276. https://doi.org/10.1021/jacs.1c02149.

(64) Horst, M.; Yang, J.; Meisner, J.; Kouznetsova, T. B.; Martínez, T. J.; Craig, S. L.; Xia, Y. Understanding the Mechanochemistry of Ladder-Type Cyclobutane Mechanophores by Single Molecule Force Spectroscopy. *J Am Chem Soc* **2021,** *143* (31), 12328–12334. https://doi.org/10.1021/jacs.1c05857.

(65) Zhang, H.; Li, X.; Lin, Y.; Gao, F.; Tang, Z.; Su, P.; Zhang, W.; Xu, Y.; Weng, W.; Boulatov, R. Multi-Modal Mechanophores Based on Cinnamate Dimers. *Nat Commun* **2017**, *8* (1), 1147. https://doi.org/10.1038/s41467-017-01412-8.

(66) Kouznetsova, T. B.; Wang, J.; Craig, S. L. Combined Constant-Force and Constant-Velocity Single-Molecule Force Spectroscopy of the Conrotatory Ring Opening Reaction of Benzocyclobutene. *Chemphyschem* **2016**, *18* (11), 1486–1489. https://doi.org/10.1002/cphc.201600463.

(67) Brantley, J. N.; Wiggins, K. M.; Bielawski, C. W. Polymer Mechanochemistry: The Design and Study of Mechanophores. *Polym Int* **2013**, *62* (1), 2–12. https://doi.org/10.1002/pi.4350.

(68) Brown, C. L.; Craig, S. L. Molecular Engineering of Mechanophore Activity for Stress-Responsive Polymeric Materials. *Chem Sci* **2015**, *6* (4), 2158–2165. https://doi.org/10.1039/c4sc01945h.

(69) Akbulatov, S.; Boulatov, R. Experimental Polymer Mechanochemistry and Its Interpretational Frameworks. *Chemphyschem* **1422**, *18* (11), 1422–1450. https://doi.org/10.1002/cphc.201601354.

(70) Kim, G.; Wu, Q.; Chu, J. L.; Smith, E. J.; Oelze, M. L.; Moore, J. S.; Li, K. C. Ultrasound Controlled Mechanophore Activation in Hydrogels for Cancer Therapy. *Proc National Acad Sci* **2022**, *119* (4), e2109791119. https://doi.org/10.1073/pnas.2109791119.

(71) Seiffert, S. Origin of Nanostructural Inhomogeneity in Polymer-Network Gels. *Polym Chem-uk* **2017**, *8* (31), 4472–4487. https://doi.org/10.1039/c7py01035d.

(72) Gu, Y.; Zhao, J.; Johnson, J. A. Polymer Networks: From Plastics and Gels to Porous Frameworks. *Angewandte Chemie Int Ed* **2020**, *59* (13), 5022–5049. https://doi.org/10.1002/anie.201902900.

(73) Danielsen, S. P. O.; Beech, H. K.; Wang, S.; El-Zaatari, B. M.; Wang, X.; Sapir, L.; Ouchi, T.; Wang, Z.; Johnson, P. N.; Hu, Y.; Lundberg, D. J.; Stoychev, G.; Craig, S. L.; Johnson, J. A.; Kalow, J. A.; Olsen, B. D.; Rubinstein, M. Molecular Characterization of Polymer Networks. *Chem Rev* **2021,** *121* (8), 5042–5092. https://doi.org/10.1021/acs.chemrev.0c01304.

(74) Grest, G. S.; Kremer, K. Statistical Properties of Random Cross-Linked Rubbers. *Macromolecules* **1990**, *23* (23), 4994–5000. https://doi.org/10.1021/ma00225a020.

(75) Tehrani, M.; Sarvestani, A. Effect of Chain Length Distribution on Mechanical Behavior of Polymeric Networks. *Eur Polym J* **2017**, *87*, 136–146. https://doi.org/10.1016/j.eurpolymj.2016.12.017.

(76) Sorichetti, V.; Ninarello, A.; Ruiz-Franco, J. M.; Hugouvieux, V.; Kob, W.; Zaccarelli, E.; Rovigatti, L. Effect of Chain Polydispersity on the Elasticity of Disordered Polymer Networks. *Macromolecules* **2021**, *54* (8), 3769–3779. https://doi.org/10.1021/acs.macromol.1c00176.

(77) Wun, K. L.; Prins, W. Assessment of Nonrandom Crosslinking in Polymer Networks by Small-angle Light Scattering. *J Polym Sci Polym Phys Ed* **1974**, *12* (3), 533–543. https://doi.org/10.1002/pol.1974.180120307.

(78) Candau, S. J.; Young, C. Y.; Tanaka, T.; Lemarechal, P.; Bastide, J. Intensity of Light Scattered from Polymeric Gels: Influence of the Structure of the Networks. *J Chem Phys* **1979**, *70* (10), 4694–4700. https://doi.org/10.1063/1.437255.

(79) Shibayama, M. Small-Angle Neutron Scattering on Polymer Gels: Phase Behavior, Inhomogeneities and Deformation Mechanisms. *Polym J* **2011**, *43* (1), 18–34. https://doi.org/10.1038/pj.2010.110.

(80) Lorenzo, F. D.; Seiffert, S. Nanostructural Heterogeneity in Polymer Networks and Gels. *Polym Chem-uk* **2015**, *6* (31), 5515–5528. https://doi.org/10.1039/c4py01677g.

(81) Bastide, J.; Leibler, L. Large-Scale Heterogeneities in Randomly Cross-Linked Networks. *Macromolecules* **1988**, *21* (8), 2647–2649. https://doi.org/10.1021/ma00186a058.

(82) Lorenzo, F. D.; Hellwig, J.; Klitzing, R. von; Seiffert, S. Macroscopic and Microscopic Elasticity of Heterogeneous Polymer Gels. *Acs Macro Lett* **2015**, *4* (7), 698–703. https://doi.org/10.1021/acsmacrolett.5b00228.

(83) Urayama, K. Network Topology–Mechanical Properties Relationships of Model Elastomers. *Polym J* **2008**, *40* (8), 669–678. https://doi.org/10.1295/polymj.pj2008033.

(84) Chassé, W.; Schlögl, S.; Riess, G.; Saalwächter, K. Inhomogeneities and Local Chain Stretching in Partially Swollen Networks. *Soft Matter* **2013**, *9* (29), 6943–6954. https://doi.org/10.1039/c3sm50195g.

(85) Schlögl, S.; Trutschel, M.-L.; Chassé, W.; Riess, G.; Saalwächter, K. Entanglement Effects in Elastomers: Macroscopic vs Microscopic Properties. *Macromolecules* **2014**, *47* (9), 2759–2773. https://doi.org/10.1021/ma4026064.

(86) Zhong, M.; Wang, R.; Kawamoto, K.; Olsen, B. D.; Johnson, J. A. Quantifying the Impact of Molecular Defects on Polymer Network Elasticity. *Science* **2016**, *353* (6305), 1264–1268. https://doi.org/10.1126/science.aag0184.

(87) Rebello, N. J.; Beech, H. K.; Olsen, B. D. Adding the Effect of Topological Defects to the Flory–Rehner and Bray–Merrill Swelling Theories. *Acs Macro Lett* **2021**, *10* (5), 531–537. https://doi.org/10.1021/acsmacrolett.0c00909.

(88) Wang, Q.; Gossweiler, G. R.; Craig, S. L.; Zhao, X. Mechanics of Mechanochemically Responsive Elastomers. *J Mech Phys Solids* **2015**, *82*, 320-344. https://doi.org/10.1016/j.jmps.2015.05.007.

(89) Eirich, F. R. Failure Modes of Elastomers. *Eng Fract Mech* **1973**, *5* (3), 555–562. https://doi.org/10.1016/0013-7944(73)90040-4.

(90) Adhikari, R.; Makarov, D. E. Mechanochemical Kinetics in Elastomeric Polymer Networks: Heterogeneity of Local Forces Results in Nonexponential Kinetics. *J Phys Chem B* **2017**, *121* (10), 2359–2365. https://doi.org/10.1021/acs.jpcb.6b12758.

(91) Dubach, F. F. C.; Ellenbroek, W. G.; Storm, C. How Accurately Do Mechanophores Report on Bond Scission in Soft Polymer Materials? *J Polym Sci* **2021,** *59* (12), 1188-1199. https://doi.org/10.1002/pol.20210025.

(92) Tian, Y.; Kucharski, T. J.; Yang, Q.-Z.; Boulatov, R. Model Studies of Force-Dependent Kinetics of Multi-Barrier Reactions. *Nat Commun* **2013**, *4* (1), 2538. https://doi.org/10.1038/ncomms3538.

(93) Tian, Y.; Boulatov, R. Quantum-Chemical Validation of the Local Assumption of Chemomechanics for a Unimolecular Reaction. *Chemphyschem* **2012**, *13* (9), 2277–2281. https://doi.org/10.1002/cphc.201200207.

(94) Huang, Z.; Boulatov, R. Chemomechanics: Chemical Kinetics for Multiscale Phenomena. *Chem Soc Rev* **2011**, *40* (5), 2359. https://doi.org/10.1039/c0cs00148a.

(95) Suzuki, Y.; Dudko, O. K. Single-Molecule Rupture Dynamics on Multidimensional Landscapes. *Phys Rev Lett* **2010**, *104* (4), 048101. https://doi.org/10.1103/physrevlett.104.048101.

(96) Liu, Y.; Holm, S.; Meisner, J.; Jia, Y.; Wu, Q.; Woods, T. J.; Martinez, T. J.; Moore, J. S. Flyby Reaction Trajectories: Chemical Dynamics under Extrinsic Force. *Science* **2021**, *373* (6551), 208–212. https://doi.org/10.1126/science.abi7609.

(97) Hamed, G. R. Molecular Aspects of the Fatigue and Fracture of Rubber. *Rubber Chem Technol* **1994**, *67* (3), 529–536. https://doi.org/10.5254/1.3538689.

(98) Arora, A.; Lin, T.-S.; Beech, H. K.; Mochigase, H.; Wang, R.; Olsen, B. D. Fracture of Polymer Networks Containing Topological Defects. *Macromolecules* **2020**, *53* (17), 7346–7355. https://doi.org/10.1021/acs.macromol.0c01038.

(99) Bueche, F.; Halpin, J. C. Molecular Theory for the Tensile Strength of Gum Elastomers. *J Appl Phys* **1964**, *35* (1), 36–41. https://doi.org/10.1063/1.1713095.

(100) Slootman, J.; Waltz, V.; Yeh, C. J.; Baumann, C.; Göstl, R.; Comtet, J.; Creton, C. Quantifying Rate- and Temperature-Dependent Molecular Damage in Elastomer Fracture. *Phys Rev X* **2020**, *10* (4), 041045. https://doi.org/10.1103/physrevx.10.041045.

(101) Wang, Z.; Zheng, X.; Ouchi, T.; Kouznetsova, T. B.; Beech, H. K.; Av-Ron, S.; Matsuda, T.; Bowser, B. H.; Wang, S.; Johnson, J. A.; Kalow, J. A.; Olsen, B. D.; Gong, J. P.; Rubinstein, M.; Craig, S. L. Toughening Hydrogels through Force-Triggered Chemical Reactions That Lengthen Polymer Strands. *Sci New York N Y* **2021**, *374* (6564), 193–196. https://doi.org/10.1126/science.abg2689.

(102) Gu, Y.; Kawamoto, K.; Zhong, M.; Chen, M.; Hore, M. J. A.; Jordan, A. M.; Korley, L. T. J.; Olsen, B. D.; Johnson, J. A. Semibatch Monomer Addition as a General Method to Tune and Enhance the Mechanics of Polymer Networks via Loop-Defect Control. *Proc National Acad Sci* **2017**, *114* (19), 4875–4880. https://doi.org/10.1073/pnas.1620985114.

(103) Gu, Y.; Schauenburg, D.; Bode, J. W.; Johnson, J. A. Leaving Groups as Traceless Topological Modifiers for the Synthesis of Topologically Isomeric Polymer Networks. *J Am Chem Soc* **2018**, *140* (43), 14033–14037. https://doi.org/10.1021/jacs.8b07967.

(104) Braunecker, W. A.; Matyjaszewski, K. Controlled/Living Radical Polymerization: Features, Developments, and Perspectives. *Prog Polym Sci* **2007**, *32* (1), 93–146. https://doi.org/10.1016/j.progpolymsci.2006.11.002.

(105) Grubbs, R. B.; Grubbs, R. H. 50th Anniversary Perspective: Living Polymerization Emphasizing the Molecule in Macromolecules. *Macromolecules* **2017**, *50* (18), 6979–6997. https://doi.org/10.1021/acs.macromol.7b01440.

(106) Ide, N.; Fukuda, T. Nitroxide-Controlled Free-Radical Copolymerization of Vinyl and Divinyl Monomers. 2. Gelation. *Macromolecules* **1999**, *32* (1), 95–99. https://doi.org/10.1021/ma9805349.

(107) Moad, G. RAFT (Reversible Addition–Fragmentation Chain Transfer) Crosslinking (Co)Polymerization of Multi-olefinic Monomers to Form Polymer Networks. *Polym Int* **2015**, *64* (1), 15–24. https://doi.org/10.1002/pi.4767.

(108) Oh, J. K.; Tang, C.; Gao, H.; Tsarevsky, N. V.; Matyjaszewski, K. Inverse Miniemulsion ATRP: A New Method for Synthesis and Functionalization of Well-Defined Water-Soluble/Cross-Linked Polymeric Particles. *J Am Chem Soc* **2006**, *128* (16), 5578–5584. https://doi.org/10.1021/ja060586a.

(109) Liu, Q.; Zhang, P.; Qing, A.; Lan, Y.; Lu, M. Poly(N-Isopropylacrylamide) Hydrogels with Improved Shrinking Kinetics by RAFT Polymerization. *Polymer* **2006**, *47* (7), 2330–2336. https://doi.org/10.1016/j.polymer.2006.02.006.

(110) Roy, S. G.; Haldar, U.; De, P. Remarkable Swelling Capability of Amino Acid Based Cross-Linked Polymer Networks in Organic and Aqueous Medium. *Acs Appl Mater Inter* **2014**, *6* (6), 4233–4241. https://doi.org/10.1021/am405932f.

(111) Webster, O. W. Living Polymerization Methods. *Science* **1991**, *251* (4996), 887–893. https://doi.org/10.1126/science.251.4996.887.

(112) Krys, P.; Matyjaszewski, K. Kinetics of Atom Transfer Radical Polymerization. *Eur Polym J* **2017**, *89*, 482–523. https://doi.org/10.1016/j.eurpolymj.2017.02.034.

(113) Perrier, S. 50th Anniversary Perspective: RAFT Polymerization A User Guide. *Macromolecules* **2017**, *50* (19), 7433–7447. https://doi.org/10.1021/acs.macromol.7b00767.

(114) Johnson, J. A.; Lewis, D. R.; Díaz, D. D.; Finn, M. G.; Koberstein, J. T.; Turro, N. J. Synthesis of Degradable Model Networks via ATRP and Click Chemistry. *J Am Chem Soc* **2006**, *128* (20), 6564–6565. https://doi.org/10.1021/ja0612910.

(115) Wang, S.; Beech, H. K.; Bowser, B. H.; Kouznetsova, T. B.; Olsen, B. D.; Rubinstein, M.; Craig, S. L. Mechanism Dictates Mechanics: A Molecular Substituent Effect in the Macroscopic Fracture of a Covalent Polymer Network. *J Am Chem Soc* **2021**, *143* (10), 3714–3718. https://doi.org/10.1021/jacs.1c00265.

(116) Hild, G. Model Networks Based on `endlinking' Processes: Synthesis, Structure and Properties. *Prog Polym Sci* **1998**, *23* (6), 1019–1149. https://doi.org/10.1016/s0079-6700(97)00055-5.

(117) Huang, X.; Nakagawa, S.; Li, X.; Shibayama, M.; Yoshie, N. A Simple and Versatile Method for the Construction of Nearly Ideal Polymer Networks. *Angew Chem-ger Edit* **2020**, *132* (24), 9733–9739. https://doi.org/10.1002/ange.202001271.

(118) Wang, R.; Johnson, J. A.; Olsen, B. D. Odd–Even Effect of Junction Functionality on the Topology and Elasticity of Polymer Networks. *Macromolecules* **2017**, *50* (6), 2556–2564. https://doi.org/10.1021/acs.macromol.6b01912.

(119) Zhukhovitskiy, A. V.; Zhong, M.; Keeler, E. G.; Michaelis, V. K.; Sun, J. E. P.; Hore, M. J. A.; Pochan, D. J.; Griffin, R. G.; Willard, A. P.; Johnson, J. A. Highly Branched and Loop-Rich Gels via Formation of Metal–Organic Cages Linked by Polymers. *Nat Chem* **2016**, *8* (1), 33–41. https://doi.org/10.1038/nchem.2390.

(120) Gu, Y.; Alt, E. A.; Wang, H.; Li, X.; Willard, A. P.; Johnson, J. A. Photoswitching Topology in Polymer Networks with Metal–Organic Cages as Crosslinks. *Nature* **2018**, *560* (7716), 65–69. https://doi.org/10.1038/s41586-018-0339-0.

(121) Zhou, H.; Woo, J.; Cok, A. M.; Wang, M.; Olsen, B. D.; Johnson, J. A. Counting Primary Loops in Polymer Gels. *Proc National Acad Sci* **2012**, *109* (47), 19119–19124. https://doi.org/10.1073/pnas.1213169109.

(122) Zhou, H.; Schön, E.-M.; Wang, M.; Glassman, M. J.; Liu, J.; Zhong, M.; Díaz, D. D.; Olsen, B. D.; Johnson, J. A. Crossover Experiments Applied to Network Formation Reactions: Improved Strategies for Counting Elastically Inactive Molecular Defects in PEG Gels and Hyperbranched Polymers. *J Am Chem Soc* **2014**, *136* (26), 9464–9470. https://doi.org/10.1021/ja5042385.

(123) Kawamoto, K.; Zhong, M.; Wang, R.; Olsen, B. D.; Johnson, J. A. Loops versus Branch Functionality in Model Click Hydrogels. *Macromolecules* **2015**, *48* (24), 8980–8988. https://doi.org/10.1021/acs.macromol.5b02243.

(124) Wang, J.; Lin, T.-S.; Gu, Y.; Wang, R.; Olsen, B. D.; Johnson, J. A. Counting Secondary Loops Is Required for Accurate Prediction of End-Linked Polymer Network Elasticity. *Acs Macro Lett* **2018**, *7* (2), 244–249. https://doi.org/10.1021/acsmacrolett.8b00008.

(125) Wang, J.; Wang, R.; Gu, Y.; Sourakov, A.; Olsen, B. D.; Johnson, J. A. Counting Loops in Sidechain-Crosslinked Polymers from Elastic Solids to Single-Chain Nanoparticles. *Chem Sci* **2019**, *10* (20), 5332–5337. https://doi.org/10.1039/c9sc01297d.

(126) Shieh, P.; Zhang, W.; Husted, K. E. L.; Kristufek, S. L.; Xiong, B.; Lundberg, D. J.; Lem, J.; Veysset, D.; Sun, Y.; Nelson, K. A.; Plata, D. L.; Johnson, J. A. Cleavable Comonomers Enable Degradable, Recyclable Thermoset Plastics. *Nature* **2020**, *583* (7817), 542–547. https://doi.org/10.1038/s41586-020-2495-2.

(127) Hart, L. F.; Hertzog, J. E.; Rauscher, P. M.; Rawe, B. W.; Tranquilli, M. M.; Rowan, S. J. Material Properties and Applications of Mechanically Interlocked Polymers. *Nat Rev Mater* **2021**, *6* (6), 508–530. https://doi.org/10.1038/s41578-021-00278-z.

(128) Kato, K.; Yasuda, T.; Ito, K. Peculiar Elasticity and Strain Hardening Attributable to Counteracting Entropy of Chain and Ring in Slide-Ring Gels. *Polymer* **2014**, *55* (10), 2614–2619. https://doi.org/10.1016/j.polymer.2014.03.022.

(129) Harada, A.; Li, J.; Kamachi, M. The Molecular Necklace: A Rotaxane Containing Many Threaded α-Cyclodextrins. *Nature* **1992**, *356* (6367), 325–327. https://doi.org/10.1038/356325a0.

(130) Wenz, G.; Keller, B. Threading Cyclodextrin Rings on Polymer Chains. *Angewandte Chemie Int Ed Engl* **1992**, *31* (2), 197–199. https://doi.org/10.1002/anie.199201971.

(131) Gennes, P.-G. de. Sliding Gels. *Phys Statistical Mech Appl* **1999**, *271* (3–4), 231–237. https://doi.org/10.1016/s0378-4371(99)00227-7.

(132) Okumura, Y.; Ito, K. The Polyrotaxane Gel: A Topological Gel by Figure-of-Eight Cross-links. *Adv Mater* **2001**, *13* (7), 485–487. https://doi.org/10.1002/1521-4095(200104)13:7<485::aid-adma485>3.0.co;2-t.

(133) Ito, K. Novel Cross-Linking Concept of Polymer Network: Synthesis, Structure, and Properties of Slide-Ring Gels with Freely Movable Junctions. *Polym J* **2007**, *39* (6), 489–499. https://doi.org/10.1295/polymj.pj2006239.

(134) Noda, Y.; Hayashi, Y.; Ito, K. From Topological Gels to Slide-ring Materials. *J Appl Polym Sci* **2014**, *131* (15), 40509. https://doi.org/10.1002/app.40509.

(135) Ito, K. Slide-Ring Materials Using Cyclodextrin. *Chem Pharm Bulletin* **2017**, *65* (4), 326–329. https://doi.org/10.1248/cpb.c16-00874.

(136) Colley, N. D.; Nosiglia, M. A.; Li, L.; Amir, F.; Chang, C.; Greene, A. F.; Fisher, J. M.; Li, R.; Li, X.; Barnes, J. C. One-Pot Synthesis of a Linear [4]Catenate Using Orthogonal Metal Templation and Ring-Closing Metathesis. *Inorg Chem* **2020**, *59* (15), 10450–10460. https://doi.org/10.1021/acs.inorgchem.0c00735.

(137) Lee, B.; Niu, Z.; Wang, J.; Slebodnick, C.; Craig, S. L. Relative Mechanical Strengths of Weak Bonds in Sonochemical Polymer Mechanochemistry. *J Am Chem Soc* **2015**, *137* (33), 10826–10832. https://doi.org/10.1021/jacs.5b06937.

(138) Wang, S.; Panyukov, S.; Rubinstein, M.; Craig, S. L. Quantitative Adjustment to the Molecular Energy Parameter in the Lake–Thomas Theory of Polymer Fracture Energy. *Macromolecules* **2019**, *52* (7), 2772–2777. https://doi.org/10.1021/acs.macromol.8b02341.

(139) Liu, C.; Kadono, H.; Yokoyama, H.; Mayumi, K.; Ito, K. Crack Propagation Resistance of Slide-Ring Gels. *Polymer* **2019**, *181*, 121782. https://doi.org/10.1016/j.polymer.2019.121782.

(140) Mayumi, K.; Ito, K.; Kato, K. *Polyrotaxane and Slide-Ring Materials*; Monographs in Supramolecular Chemistry; Royal Society of Chemistry: Cambridge, UK, 2015. https://doi.org/10.1039/9781782622284.

(141) Liu, C.; Morimoto, N.; Jiang, L.; Kawahara, S.; Noritomi, T.; Yokoyama, H.; Mayumi, K.; Ito, K. Tough Hydrogels with Rapid Self-Reinforcement. *Science* **2021**, *372* (6546), 1078–1081. https://doi.org/10.1126/science.aaz6694.

(142) Chen, C.; Wang, Z.; Suo, Z. Flaw Sensitivity of Highly Stretchable Materials. *Extreme Mech Lett* **2017**, *10*, 50–57. https://doi.org/10.1016/j.eml.2016.10.002.

(143) Gong, J. P.; Katsuyama, Y.; Kurokawa, T.; Osada, Y. Double-Network Hydrogels with Extremely High Mechanical Strength. *Adv Mater* **2003**, *15* (14), 1155–1158. https://doi.org/10.1002/adma.200304907.

(144) Ducrot, E.; Chen, Y.; Bulters, M.; Sijbesma, R. P.; Creton, C. Toughening Elastomers with Sacrificial Bonds and Watching Them Break. *Science* **2014**, *344* (6180), 186–189. https://doi.org/10.1126/science.1248494.

(145) Millereau, P.; Ducrot, E.; Clough, J. M.; Wiseman, M. E.; Brown, H. R.; Sijbesma, R. P.; Creton, C. Mechanics of Elastomeric Molecular Composites. *Proc National Acad Sci* **2018**, *115* (37), 201807750. https://doi.org/10.1073/pnas.1807750115.

(146) Chen, Y.; Sanoja, G.; Creton, C. Mechanochemistry Unveils Stress Transfer during Sacrificial Bond Fracture of Tough Multiple Network Elastomers. *Chem Sci* **2021,** *12* (33), 11098-11108. https://doi.org/10.1039/d1sc03352b.

(147) Bacca, M.; Creton, C.; McMeeking, R. M. A Model for the Mullins Effect in Multinetwork Elastomers. *J Appl Mech* **2017**, *84* (12), 121009. https://doi.org/10.1115/1.4037881.

(148) Nakajima, T. Generalization of the Sacrificial Bond Principle for Gel and Elastomer Toughening. *Polym J* **2017**, *49* (6), 477–485. https://doi.org/10.1038/pj.2017.12.

(149) Nonoyama, T.; Gong, J. P. Tough Double Network Hydrogel and Its Biomedical Applications. *Annu Rev Chem Biomol* **2021**, *12* (1), 1–18. https://doi.org/10.1146/annurev-chembioeng-101220-080338.

(150) Sun, X.; Liang, Y.; Ye, L.; Liang, H. An Extremely Tough and Ionic Conductive Natural-Polymer-Based Double Network Hydrogel. *J Mater Chem B* **2021**, *9* (37), 7751–7759. https://doi.org/10.1039/d1tb01458g.

(151) Webber, R. E.; Creton, C.; Brown, H. R.; Gong, J. P. Large Strain Hysteresis and Mullins Effect of Tough Double-Network Hydrogels. *Macromolecules* **2007**, *40* (8), 2919–2927. https://doi.org/10.1021/ma062924y.

(152) Tanaka, Y.; Kawauchi, Y.; Kurokawa, T.; Furukawa, H.; Okajima, T.; Gong, J. P. Localized Yielding Around Crack Tips of Double-Network Gels. *Macromol Rapid Comm* **2008**, *29* (18), 1514–1520. https://doi.org/10.1002/marc.200800227.

(153) Yu, Q. M.; Tanaka, Y.; Furukawa, H.; Kurokawa, T.; Gong, J. P. Direct Observation of Damage Zone around Crack Tips in Double-Network Gels. *Macromolecules* **2009**, *42* (12), 3852–3855. https://doi.org/10.1021/ma900622s.

(154) Matsuda, T.; Kawakami, R.; Nakajima, T.; Gong, J. P. Crack Tip Field of a Double-Network Gel: Visualization of Covalent Bond Scission through Mechanoradical Polymerization. *Macromolecules* **2020**, *53* (20), 8787–8795. https://doi.org/10.1021/acs.macromol.0c01485.

(155) Chen, Y.; Yeh, C. J.; Qi, Y.; Long, R.; Creton, C. From Force-Responsive Molecules to Quantifying and Mapping Stresses in Soft Materials. *Sci Adv* **2020**, *6* (20), eaaz5093. https://doi.org/10.1126/sciadv.aaz5093.

(156) Chen, Y.; Yeh, C. J.; Guo, Q.; Qi, Y.; Long, R.; Creton, C. Fast Reversible Isomerization of Merocyanine as a Tool to Quantify Stress History in Elastomers. *Chem Sci* **2020**, *12* (5), 1693–1701. https://doi.org/10.1039/d0sc06157c.

(157) Tanaka, Y. A Local Damage Model for Anomalous High Toughness of Double-Network Gels. *Europhys Lett* **2007**, *78* (5), 56005. https://doi.org/10.1209/0295-5075/78/56005.

(158) Brown, H. R. A Model of the Fracture of Double Network Gels. *Macromolecules* **2007**, *40* (10), 3815–3818. https://doi.org/10.1021/ma062642y.

(159) Watabe, T.; Aoki, D.; Otsuka, H. Polymer-Network Toughening and Highly Sensitive Mechanochromism via a Dynamic Covalent Mechanophore and a Multinetwork Strategy. *Macromolecules* **2022**, *55* (13), 5795–5802. https://doi.org/10.1021/acs.macromol.2c00724.

(160) Na, Y.-H.; Tanaka, Y.; Kawauchi, Y.; Furukawa, H.; Sumiyoshi, T.; Gong, J. P.; Osada, Y. Necking Phenomenon of Double-Network Gels. *Macromolecules* **2006**, *39* (14), 4641–4645. https://doi.org/10.1021/ma060568d.

(161) Gong, J. P. Why Are Double Network Hydrogels so Tough? *Soft Matter* **2010**, *6* (12), 2583–2590. https://doi.org/10.1039/b924290b.

(162) Sagara, Y.; Karman, M.; Verde-Sesto, E.; Matsuo, K.; Kim, Y.; Tamaoki, N.; Weder, C. Rotaxanes as Mechanochromic Fluorescent Force Transducers in Polymers. *J Am Chem Soc* **2018**, *140* (5), 1584–1587. https://doi.org/10.1021/jacs.7b12405.

(163) Sagara, Y.; Karman, M.; Seki, A.; Pannipara, M.; Tamaoki, N.; Weder, C. Rotaxane-Based Mechanophores Enable Polymers with Mechanically Switchable White Photoluminescence. *Acs Central Sci* **2019**, *5* (5), 874–881. https://doi.org/10.1021/acscentsci.9b00173.

(164) Ouchi, T.; Bowser, B. H.; Kouznetsova, T. B.; Zheng, X.; Craig, S. L. Strain-Triggered Acidification in a Double-Network Hydrogel Enabled by Multi-Functional Transduction of Molecular Mechanochemistry. *Materials Horizons* **2023**. https://doi.org/10.1039/d2mh01105k.

(165) Oka, H.; Imato, K.; Sato, T.; Ohishi, T.; Goseki, R.; Otsuka, H. Enhancing Mechanochemical Activation in the Bulk State by Designing Polymer Architectures. *Acs Macro Lett* **2016**, *5* (10), 1124–1127. https://doi.org/10.1021/acsmacrolett.6b00529.

(166) Watabe, T.; Ishizuki, K.; Aoki, D.; Otsuka, H. Mechanochromic Dendrimers: The Relationship between Primary Structure and Mechanochromic Properties in the Bulk. *Chem Commun* **2019**, *55* (48), 6831–6834. https://doi.org/10.1039/c9cc03011e.

(167) Watabe, T.; Aoki, D.; Otsuka, H. Enhancement of Mechanophore Activation in Mechanochromic Dendrimers by Functionalization of Their Surface. *Macromolecules* **2021,** *54* (4), 1725–1731. https://doi.org/10.1021/acs.macromol.0c02497.

(168) Zhang, M.; Bo, G. D. Impact of a Mechanical Bond on the Activation of a Mechanophore. *J Am Chem Soc* **2018**, *140* (40), 12724–12727. https://doi.org/10.1021/jacs.8b08590.

(169) Lu, Y.; Aoki, D.; Sawada, J.; Kosuge, T.; Sogawa, H.; Otsuka, H.; Takata, T. Visualization of the Slide-Ring Effect: A Study on Movable Cross-Linking Points Using Mechanochromism. *Chem Commun* **2020**, *56* (23), 3361–3364. https://doi.org/10.1039/c9cc09452k.

(170) Qiu, W.; Gurr, P. A.; Qiao, G. G. Regulating Color Activation Energy of Mechanophore-Linked Multinetwork Elastomers. *Macromolecules* **2020**, *53* (10), 4090–4098. https://doi.org/10.1021/acs.macromol.0c00477.

(171) Wang, L.-J.; Yang, K.-X.; Zhou, Q.; Yang, H.-Y.; He, J.-Q.; Zhang, X.-Y. Rhodamine Mechanophore Functionalized Mechanochromic Double Network Hydrogels with High Sensitivity to Stress. *Chinese J Polym Sci* **2020**, *38* (1), 24–36. https://doi.org/10.1007/s10118-019-2293-1.

(172) Wang, L.; Zhou, W.; Tang, Q.; Yang, H.; Zhou, Q.; Zhang, X. Rhodamine-Functionalized Mechanochromic and Mechanofluorescent Hydrogels with Enhanced Mechanoresponsive Sensitivity. *Polymers-basel* **2018**, *10* (9), 994. https://doi.org/10.3390/polym10090994.

(173) Zhang, H.; Zeng, D.; Pan, Y.; Chen, Y.; Ruan, Y.; Xu, Y.; Boulatov, R.; Creton, C.; Weng, W. Mechanochromism and Optical Remodeling of Multi-Network Elastomers Containing Anthracene Dimers. *Chem Sci* **2019**, *10* (36), 8367–8373. https://doi.org/10.1039/c9sc02580d.

(174) Wang, Z. J.; Jiang, J.; Mu, Q.; Maeda, S.; Nakajima, T.; Gong, J. P. Azo-Crosslinked Double-Network Hydrogels Enabling Highly Efficient Mechanoradical Generation. *J Am Chem Soc* **2022**, *144* (7), 3154–3161. https://doi.org/10.1021/jacs.1c12539.

(175) Akiba, M.; Hashim, A. S. Vulcanization and Crosslinking in Elastomers. *Prog Polym Sci* **1997**, *22* (3), 475–521. https://doi.org/10.1016/s0079-6700(96)00015-9.

(176) Coquillat, M.; Verdu, J.; Colin, X.; Audouin, L.; Nevière, R. Thermal Oxidation of Polybutadiene. Part 2: Mechanistic and Kinetic Schemes for Additive-Free Non-Crosslinked Polybutadiene. *Polym Degrad Stabil* **2007**, *92* (7), 1334–1342. https://doi.org/10.1016/j.polymdegradstab.2007.03.019.

(177) Wang, C.; Akbulatov, S.; Chen, Q.; Tian, Y.; Sun, C.-L.; Couty, M.; Boulatov, R. The Molecular Mechanism of Constructive Remodeling of a Mechanically-Loaded Polymer. *Nat Commun* **2022**, *13* (1), 3154. https://doi.org/10.1038/s41467-022-30947-8.

(178) Nakajima, T.; Fukuda, Y.; Kurokawa, T.; Sakai, T.; Chung, U.; Gong, J. P. Synthesis and Fracture Process Analysis of Double Network Hydrogels with a Well-Defined First Network. *Acs Macro Lett* **2013**, *2* (6), 518–521. https://doi.org/10.1021/mz4002047.

(179) Jiang, Y.; Korpas, L. M.; Raney, J. R. Bifurcation-Based Embodied Logic and Autonomous Actuation. *Nat Commun* **2019**, *10* (1), 128. https://doi.org/10.1038/s41467-018-08055-3.

(180) Yasuda, H.; Korpas, L. M.; Raney, J. R. Transition Waves and Formation of Domain Walls in Multistable Mechanical Metamaterials. *Phys Rev Appl* **2020**, *13* (5), 054067. https://doi.org/10.1103/physrevapplied.13.054067.

TOC Graphic

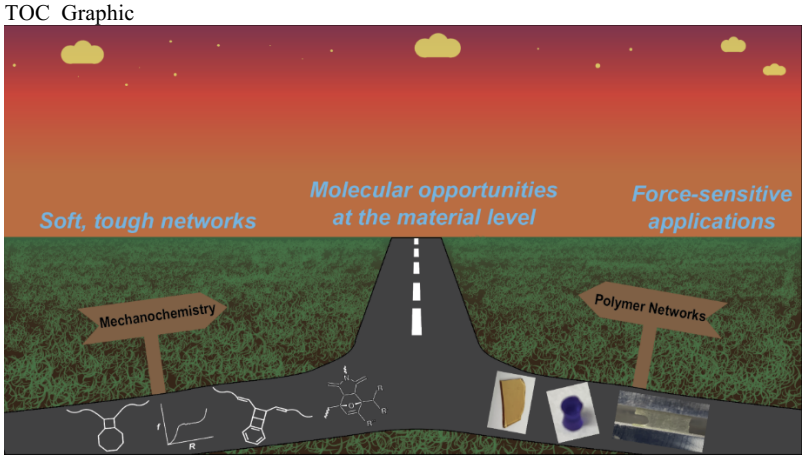
Soft, tough networks
Molecular opportunities at the material level
Force-sensitive applications
Mechanochemistry
Polymer Networks